JOURNAL OF VIROLOGY, Dec. 2011, p. 13185–13194 Vol. 85, No. 24
0022-538X/11/$12.00 doi:10.1128/JVI.06099-11

Dysfunction of Autophagy Participates in Vacuole Formation and Cell Death in Cells Replicating Hepatitis C Virus▽§

Shuhei Taguwa,[1]† Hiroto Kambara,[1]† Naonobu Fujita,[2] Takeshi Noda,[2] Tamotsu Yoshimori,[2] Kazuhiko Koike,[3] Kohji Moriishi,[4] and Yoshiharu Matsuura[1]*

Department of Molecular Virology, Research Institute for Microbial Diseases,[1] and Department of Genetics, Graduate School of Medicine,[2] Osaka University, Osaka 565-0871, Department of Gastroenterology, Graduate School of Medicine, University of Tokyo, Tokyo 113-8655,[3] and Department of Microbiology, Faculty of Medicine, Yamanashi University, Yamanashi 409-3898,[4] Japan

Received 22 August 2011/Accepted 4 October 2011

Hepatitis C virus (HCV) is a major cause of chronic liver diseases. A high risk of chronicity is the major concern of HCV infection, since chronic HCV infection often leads to liver cirrhosis and hepatocellular carcinoma. Infection with the HCV genotype 1 in particular is considered a clinical risk factor for the development of hepatocellular carcinoma, although the molecular mechanisms of the pathogenesis are largely unknown. Autophagy is involved in the degradation of cellular organelles and the elimination of invasive microorganisms. In addition, disruption of autophagy often leads to several protein deposition diseases. Although recent reports suggest that HCV exploits the autophagy pathway for viral propagation, the biological significance of the autophagy to the life cycle of HCV is still uncertain. Here, we show that replication of HCV RNA induces autophagy to inhibit cell death. Cells harboring an HCV replicon RNA of genotype 1b strain Con1 but not of genotype 2a strain JFH1 exhibited an incomplete acidification of the autolysosome due to a lysosomal defect, leading to the enhanced secretion of immature cathepsin B. The suppression of autophagy in the Con1 HCV replicon cells induced severe cytoplasmic vacuolation and cell death. These results suggest that HCV harnesses autophagy to circumvent the harmful vacuole formation and to maintain a persistent infection. These findings reveal a unique survival strategy of HCV and provide new insights into the genotype-specific pathogenicity of HCV.

Hepatitis C virus (HCV) is a major causative agent of bloodborne hepatitis and currently infects at least 180 million people worldwide (58). The majority of individuals infected with HCV develop chronic hepatitis, which eventually leads to liver cirrhosis and hepatocellular carcinoma (25, 48). In addition, HCV infection is known to induce extrahepatic diseases such as type 2 diabetes and malignant lymphoma (20). It is believed that the frequency of development of these diseases varies among viral genotypes (14, 51). However, the precise mechanism of the genotype-dependent outcome of HCV-related diseases has not yet been elucidated. Despite HCV's status as a major public health problem, the current therapy with pegylated interferon and ribavirin is effective in only around 50% of patients with genotype 1, which is the most common genotype worldwide, and no effective vaccines for HCV are available (35, 52). Although recently approved protease inhibitors for HCV exhibited a potent antiviral efficacy in patients with genotype 1 (36, 43), the emergence of drug-resistant mutants is a growing problem (16). Therefore, it is important to clarify the life cycle and pathogenesis of HCV for the development of more potent remedies for chronic hepatitis C.

* Corresponding author. Mailing address: Department of Molecular Virology, Research Institute for Microbial Diseases, Osaka University, 3-1, Yamadaoka, Suita-shi, Osaka 565-0871, Japan. Phone: 81-6-6879-8340. Fax: 81-6-6879-8269. E-mail: matsuura@biken.osaka-u.ac.jp.
† These authors contributed equally to this work.
§ Supplemental material for this article may be found at http://jvi.asm.org/.
▽ Published ahead of print on 12 October 2011.

HCV belongs to the genus *Hepacivirus* of the family *Flaviviridae* and possesses a single positive-stranded RNA genome with a nucleotide length of 9.6 kb, which encodes a single polyprotein consisting of approximately 3,000 amino acids (40). The precursor polyprotein is processed by host and viral proteases into structural and nonstructural (NS) proteins (34). Not only viral proteins but also several host factors are required for efficient replication of the HCV genome, where NS5A is known to recruit various host proteins and to form replication complexes with other NS proteins (39). In the HCV-propagating cell, host intracellular membranes are reconstructed for the viral niche known as the membranous web, where it is thought that progeny viral RNA and proteins are concentrated for efficient replication and are protected from defensive degradation, as are the host protease and nucleases (38).

Autophagy is a bulk degradation process, wherein portions of cytoplasm and organelles are enclosed by a unique membrane structure called an autophagosome, which subsequently fuses with the lysosome for degradation (37, 60). Autophagy occurs not only in order to recycle amino acids during starvation but also to clear away deteriorated proteins or organelles irrespective of nutritional stress. In fact, the deficiency of autophagy leads to the accumulation of disordered proteins that can ultimately cause a diverse range of diseases, including neurodegeneration and liver injury (12, 29, 30), and often to type 2 diabetes and malignant lymphoma (9, 32).

Recently, it has been shown that autophagy is provoked upon replication of several RNA viruses and is closely related to their propagation and/or pathogenesis. Coxsackievirus B3

utilizes autophagic membrane as a site of genome replication, whereas influenza virus attenuates apoptosis through the induction of autophagy (10, 59). Moreover, several groups have reported that HCV induces autophagy for infection or replication (5, 49); however, the role(s) of autophagy in the propagation of HCV is still controversial and the involvement of autophagy in the pathogenesis of HCV has not yet been clarified. In this study, we examined the biological significance of the autophagy observed in cells in which the HCV genome replicates.

MATERIALS AND METHODS

Plasmids. The plasmids pmStrawberry-C1, pmStrawberry-Atg4B^{C74A}, pmRFP-GFP-LC3, pEGFP-LC3, and pEGFP-Atg16L were described previously (7, 8, 24). The plasmids pFGR-JFH1 and pSGR-JFH1 were kind gifts from T. Wakita.

Cell culture. All cell lines were cultured at 37°C under a humidified atmosphere with 5% CO_2. Huh7 cells were cultivated in Dulbecco's modified Eagle's medium (DMEM) supplemented with 10% fetal bovine serum (FBS), nonessential amino acids, 100 U/ml penicillin, and 100 mg/ml streptomycin. For the starvation, the cells were cultivated with Earle's balanced salt solution (EBSS) (Sigma) for 6 h. HCV replicon cells were established as described previously (53). The plasmid pairs pFK-I$_{389}$ neo/NS3-3′/NK5.1 and pFK-I$_{389}$ neo/FGR/NK5.1 and pFGR-JFH1 and pSGR-JFH1 were linearized with ScaI or XbaI. The plasmids pFGR-JFH1 and pSGR-JFH1 were treated with mung bean exonuclease. The linearized DNA was transcribed *in vitro* by using the MEGAscript T7 kit (Applied Biosystems) according to the manufacturer's protocol. The transcribed RNA was electroporated into cells under conditions of 270 V and 960 mF using a Gene Pulser (Bio-Rad). All HCV replicon cells were maintained in DMEM containing 10% FBS, nonessential amino acids, and 1 mg/ml G418 (Nacalai).

Reagents and antibodies. Concanamycin A and bafilomycin A1 were purchased from Sigma and Fluka, respectively. E64D and pepstatin A were from Peptide Institute Inc. Rabbit anti-HCV NS5A polyclonal antibody was described previously (45). Mouse monoclonal anti-JEV NS3 antibody was prepared by immunization using the recombinant protein spanning amino acid residues 171 to 619 of JEV NS3. Rabbit polyclonal anti-LC3 (PM036), mouse monoclonal anti-RFP (8D6), and anti-62/SQSTM1 (5F2) antibodies were purchased from Medical & Biological Laboratories. Rabbit polyclonal anti-cathepsin B (FL-339) and mouse monoclonal anti-LAMP1 (H4A3) antibodies were from Santa Cruz Biotechnology. Mouse monoclonal anti-HCV NS5A (HCM-131-5), rabbit polyclonal anti-β-actin, and mouse monoclonal anti-Golgin97 (CDF4) antibodies were from Austral Biologicals, Sigma, and Invitrogen, respectively. Mouse monoclonal and rabbit polyclonal anti-cathepsin B antibodies were from Calbiochem. Mouse monoclonal anti-p62/SQSTM1 (5F2) and anti-ATP6V0D1 (ab56441) antibodies were from Abcam. Rabbit polyclonal anti-Atg4B antibody was from Sigma. Mouse anti-double-stranded RNA (dsRNA) IgG2a (J2 and K1) antibodies were from Biocenter Ltd. (Szirak, Hungary).

Transfection, infection, and immunoblotting. Transfection and infection were carried out as described previously (53). Each lysosome-enriched fraction was isolated by using the Lysosome Enrichment Kit for Tissue and Cultured Cells (Pierce) according to the manufacturer's protocol. Samples were subjected to 12.5% sodium dodecyl sulfate-polyacrylamide gel electrophoresis. The proteins were transferred to polyvinylidene difluoride membranes (Millipore) and were reacted with the appropriate antibodies. The immune complexes were visualized with Super Signal West Femto substrate (Pierce) and detected by an LAS-3000 image analyzer system (Fujifilm). The protein bands of LC3 and β-actin were quantified by Multi Gauge software (Fujifilm), and the values of LC3 were normalized to those of β-actin.

Fluorescence microscopy. Cells were cultured on glass slides and then fixed with 4% paraformaldehyde in phosphate-buffered saline (PBS) at room temperature for 30 min. After being washed twice with PBS, the cells were permeabilized at room temperature for 20 min with PBS containing 0.25% saponin and then blocked with PBS containing 0.2% gelatin (gelatin-PBS) for 60 min at room temperature. The cells were incubated with gelatin-PBS containing appropriate antibodies at 37°C for 60 min and washed three times with PBS containing 1% Tween 20 (PBST). The resulting cells were incubated with gelatin-PBS containing corresponding fluorescent-conjugated secondary antibodies at 37°C for 60 min and then washed three times with PBST. The stained cells were covered with Vectashield mounting medium containing DAPI (4′,6-diamidino-2-phenylindole) (Vector Laboratories Inc.) and observed with a FluoView FV1000 laser scanning confocal microscope (Olympus). Time-lapse video microscopy was performed at 37°C with a DeltaVision microscope system (Applied Precision Inc.) equipped with a ΔTC3 culture dish system (Bioptechs) for temperature control.

Quantification of pro-cathepsin B. Each cell line was seeded on 12-well type I collagen-coated dishes (IWAKI) and cultured for 48 h. The supernatant and the cells were harvested and subjected to quantification of pro-cathepsin B by using Quantikine human pro-cathepsin B immunoassay (R&D Systems) according to the manufacturer's protocol.

Statistical analysis. Estimated values were represented as the means ± standard deviations. The significance of differences in the means was determined by Student's *t* test.

RESULTS

Autophagy is induced in the HCV replicating cell in a strain-dependent manner. To determine whether autophagy is induced during the replication of HCV, we investigated the phosphoethanolamine (PE) conjugation of LC3 in HCV replicon cells in which HCV RNA was autonomously replicating. As shown in Fig. 1A, the amounts of PE-conjugated LC-3 (LC3-II), a conventional marker for an autophagosomal membrane, in Huh7 cells were slightly increased by starvation, in conjunction with a reduction of the unmodified LC-3 (LC3-I). In contrast, the amount of LC3-II was significantly increased in the subgenomic and full genomic HCV replicon cells of the genotype 1b strain Con1 (SGR^{Con1} and FGR^{Con1}), whereas a small amount of LC3-II was detected in the full genomic replicon cells of the genotype 2a strain JFH1 (FGR^{JFH1}). We also examined the subcellular localization of LC3 by using confocal microscopy. Although LC3 was diffusely detected in the cytoplasm of naïve Huh7 cells, small foci of the accumulated LC3 appeared after starvation (Fig. 1B), whereas many LC3 foci that were larger in size than those in the starved cells appeared in the cytoplasm, particularly near the nucleus, in both SGR^{Con1} and FGR^{Con1} cells. However, a low level of LC3 focus formation comparable to that in the starved cells was observed in the FGR^{JFH1} cells. Most of the LC3 foci were not colocalized with NS5A, an HCV protein of the viral replication complex, in the HCV replicon cells, as reported previously (49). Elimination of HCV RNA from the SGR^{Con1} cells by treatment with alpha interferon (SGR^{cured}) abrogated the lipidation and accumulation of LC3 (Fig. 1C and D). Interestingly, overexpression of the HCV polyprotein of genotype 1b by an expression plasmid induced no autophagy (data not shown), suggesting that replication of viral RNA is required for induction of autophagy. Furthermore, neither lipidation nor accumulation of LC3 was observed in SGR^{JEV} cells harboring subgenomic replicon RNA cells of Japanese encephalitis virus (JEV), which is also a member of the family *Flaviviridae* (Fig. 1C and D). These results suggest that replication of HCV but not that of JEV induces autophagy.

The autophagy flux is impaired in the replicon cells of HCV strain Con1 after a step of autophagosome formation. To further examine the autophagy induced in the HCV replicon cells in more detail, Huh7 and SGR^{Con1} cells were treated with pepstatin A and E64D, inhibitors of aspartic protease and cysteine protease, respectively. In this assay, treatment of intact cells capable of inducing autophagy with the inhibitors increases the amount of LC3-II, whereas no increase is observed in cells impaired in the autophagic degradation. The amount of LC3-II was significantly increased in the naïve Huh7

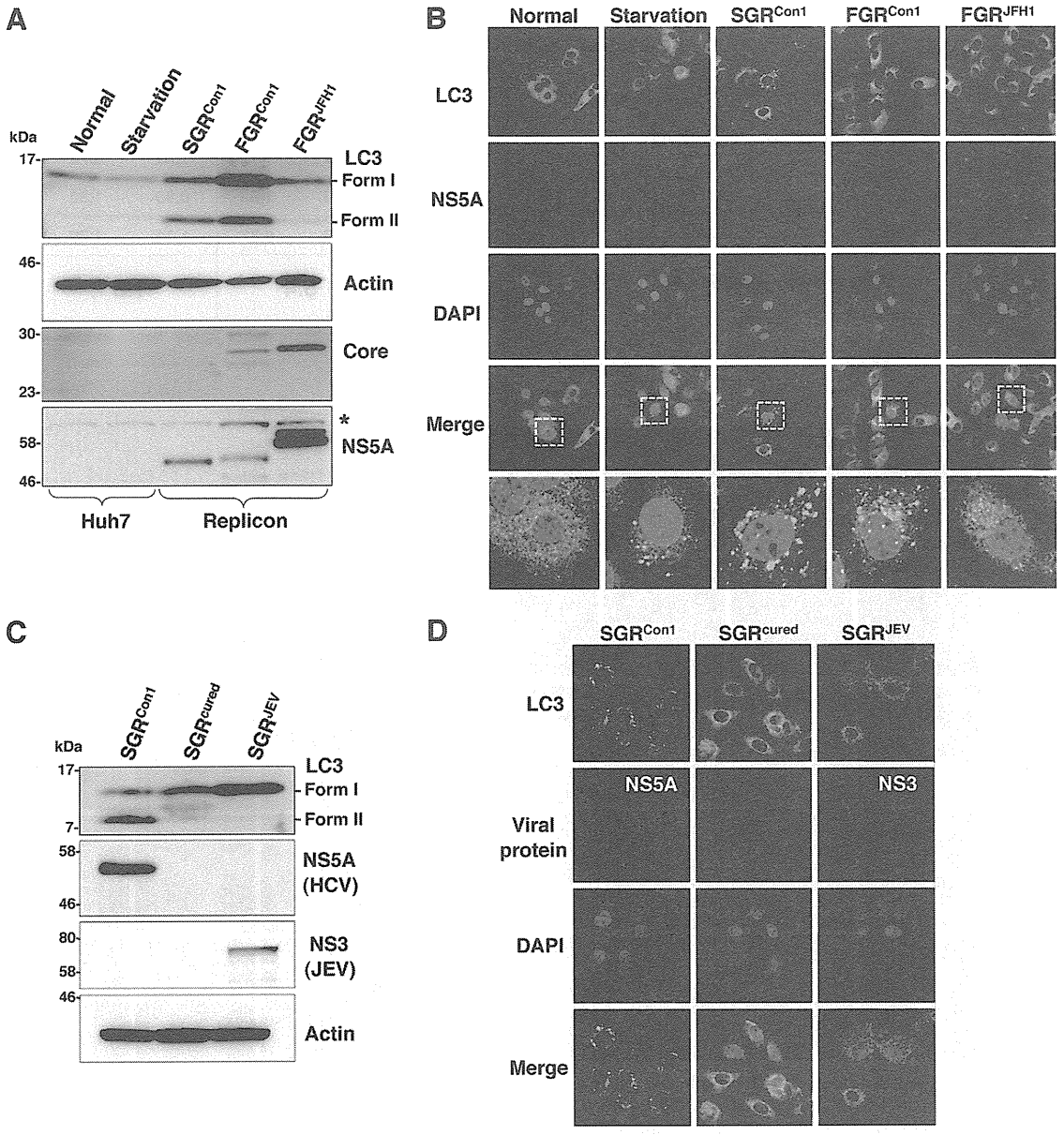

FIG. 1. Induction of autophagy in the HCV replicon cells. (A) The starved Huh7 cells and HCV replicon cells harboring a sub- or full genomic RNA of strain Con1 or strain JFH1 were subjected to immunoblotting using the appropriate antibodies. The asterisk indicates a nonspecific band. (B) Subcellular localizations of LC3 and NS5A were determined by confocal microscopy. The replicon cells and the starved Huh7 cells were stained with DAPI and then reacted with rabbit polyclonal anti-LC3 and mouse monoclonal anti-NS5A antibodies, respectively, followed by Alexa Fluor 488- and 594-conjugated secondary antibodies, respectively. The boxed areas in the merged images are magnified. (C) SGR^{Con1} cells were treated with alpha interferon for 1 week to remove the HCV replicon RNA. The resulting cells were designated SGR^{cured} cells. The SGR^{Con1}, SGR^{cured}, and SGR^{JEV} cells were lysed and subjected to immunoblotting using the appropriate antibodies. (D) Subcellular localization of LC3 and JEV NS3 and HCV NS5A was determined by confocal microscopy after staining with DAPI, followed by staining with rabbit polyclonal anti-LC3 and anti-JEV NS3 antibodies and mouse monoclonal anti-NS5A antibodies and then with the appropriate secondary antibodies. The data shown are representative of three independent experiments.

cells by treatment with the inhibitors, whereas only a slight increase was observed in the SGR^{Con1} cells (5.4-fold versus 1.6-fold) (Fig. 2A), suggesting that autophagy is suppressed in the HCV replicon cells. Furthermore, cytoplasmic accumulation of LC3 was significantly increased in the naïve Huh7 cells by treatment with the inhibitors, in contrast to the only slight increase induced by treatment in the SGR^{Con1} cells (Fig. 2B). In SGR^{Con1} cells, the LC3 foci were colocalized with the polyubiquitin-binding protein p62/SQSTM1, a specific substrate for autophagy (18), suggesting that most of the autophagosomes were distributed in the cytoplasm of the SGR^{Con1} cells (Fig. 2B and C). Next, to examine the autophagy flux in the SGR^{Con1} cells, we monitored the green fluorescent protein (GFP)-conjugated LC3 dynamics in living cells by using time-lapse imaging techniques (see movies in the supplemental material). A large number of small GFP-LC3 foci were detected in the

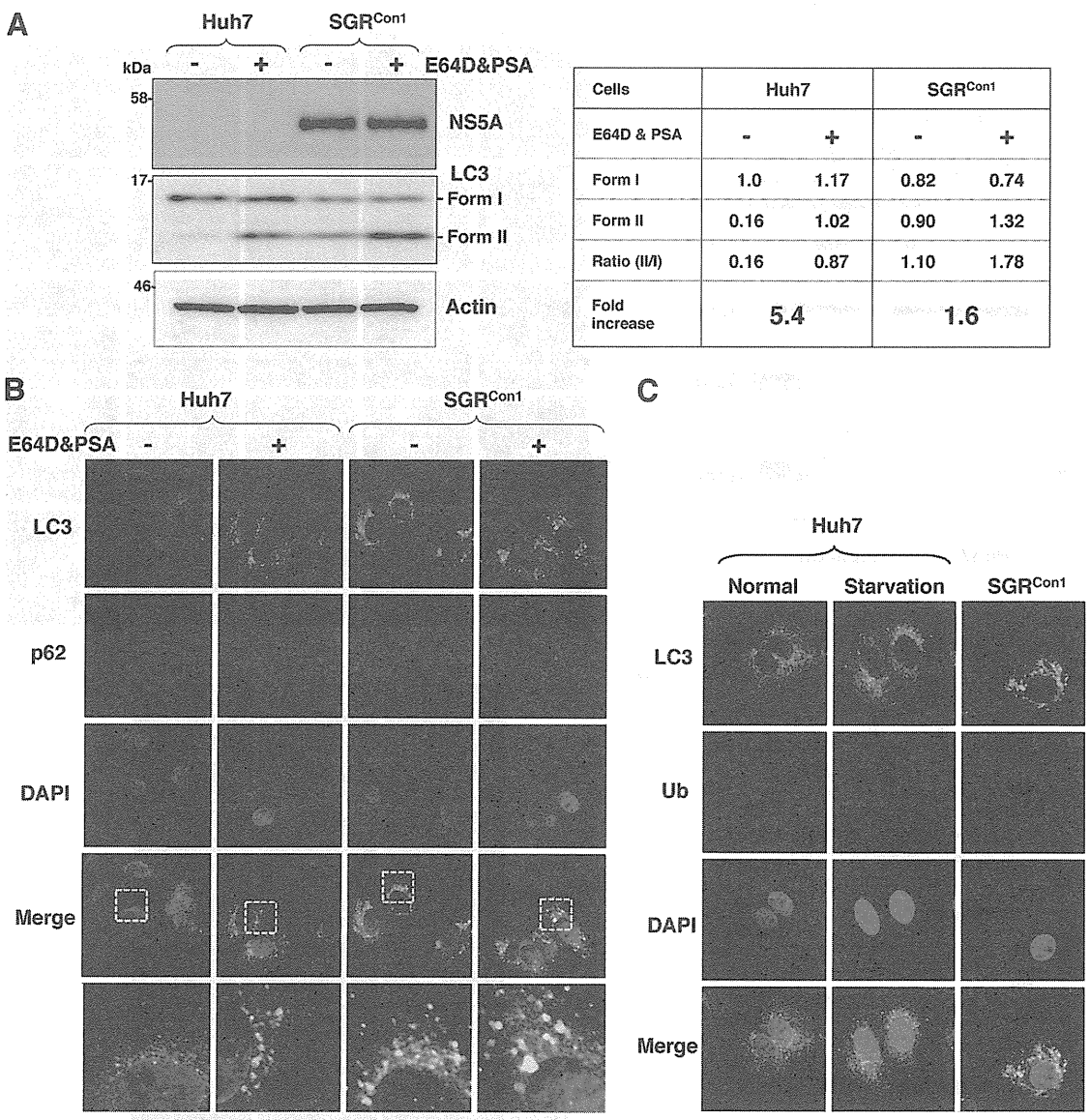

Cells	Huh7		SGR^{Con1}	
E64D & PSA	-	+	-	+
Form I	1.0	1.17	0.82	0.74
Form II	0.16	1.02	0.90	1.32
Ratio (II/I)	0.16	0.87	1.10	1.78
Fold increase	5.4		1.6	

FIG. 2. Autophagy flux is impaired in the HCV replicon cells. Autophagy flux assay using lysosomal protease inhibitors. (A) Huh7 and SGR^{Con1} cells were treated with 20 μM E64D and pepstatin A (PSA) for 6 h, and the cell lysates were subjected to immunoblotting. The density of the protein band was estimated by Multi Gauge version 2.2 (Fujifilm). (B) After nuclear staining with DAPI, the intracellular localizations of LC3 and p62 in each cell were determined by staining with rabbit polyclonal anti-LC3 and mouse monoclonal anti-62 antibodies, respectively, followed by staining with Alexa Fluor 488- and 594-conjugated secondary antibodies, respectively. The resulting cells were observed by confocal microscopy. (C) Colocalization of accumulated LC3 with ubiquitinated proteins (Ub) in SGR^{Con1} cells. Nontreated and starved Huh7 cells and SGR^{Con1} cells were fixed and stained with DAPI and rabbit anti-LC3 and anti-ubiquitin (6C1.17) (BD) polyclonal antibodies, respectively, and then with the appropriate secondary antibodies. Subcellular localizations of LC3 and Ub were determined by confocal microscopy. The data shown are representative of three independent experiments.

starved Huh7 cell, moved quickly, and finally disappeared within 30 min. Although small foci of GFP-LC3 exhibited characteristics similar to those in the starved cells, some large foci exhibited confined movement and maintained constant fluorescence for at least 3 h in the SGR^{Con1} cells. The GFP-LC3 foci in the SGR^{JFH1} cells showed characteristics similar to those in the starved cells. These results support the notion that autophagy flux is suppressed in the SGR^{Con1} cells at some step after autophagosome formation.

Impairment of autolysosomal acidification causes incomplete autophagy in the replicon cell of strain Con1. Recent studies have shown that some viruses inhibit the autophagy pathway by blocking the autolysosome formation (10, 42). Therefore, we determined the autolysosome formation in the HCV replicon cells through the fusion of autophagosome with lysosome. Colocalization of small foci of LC3 with LAMP1, a lysosome marker, was observed in the starved Huh7 cells, SGR^{Con1} cells, and SGR^{JFH1} cells but not in the SGR^{cured} cells (Fig. 3A), suggesting that autolysosomes are formed in the HCV replicon cells of both Con1 and JFH1 strains. The autolysosome is acidified by the vacuolar-type H^+ ATPase (V-ATPase) and degrades substrates by the lysosomal acidic hy-

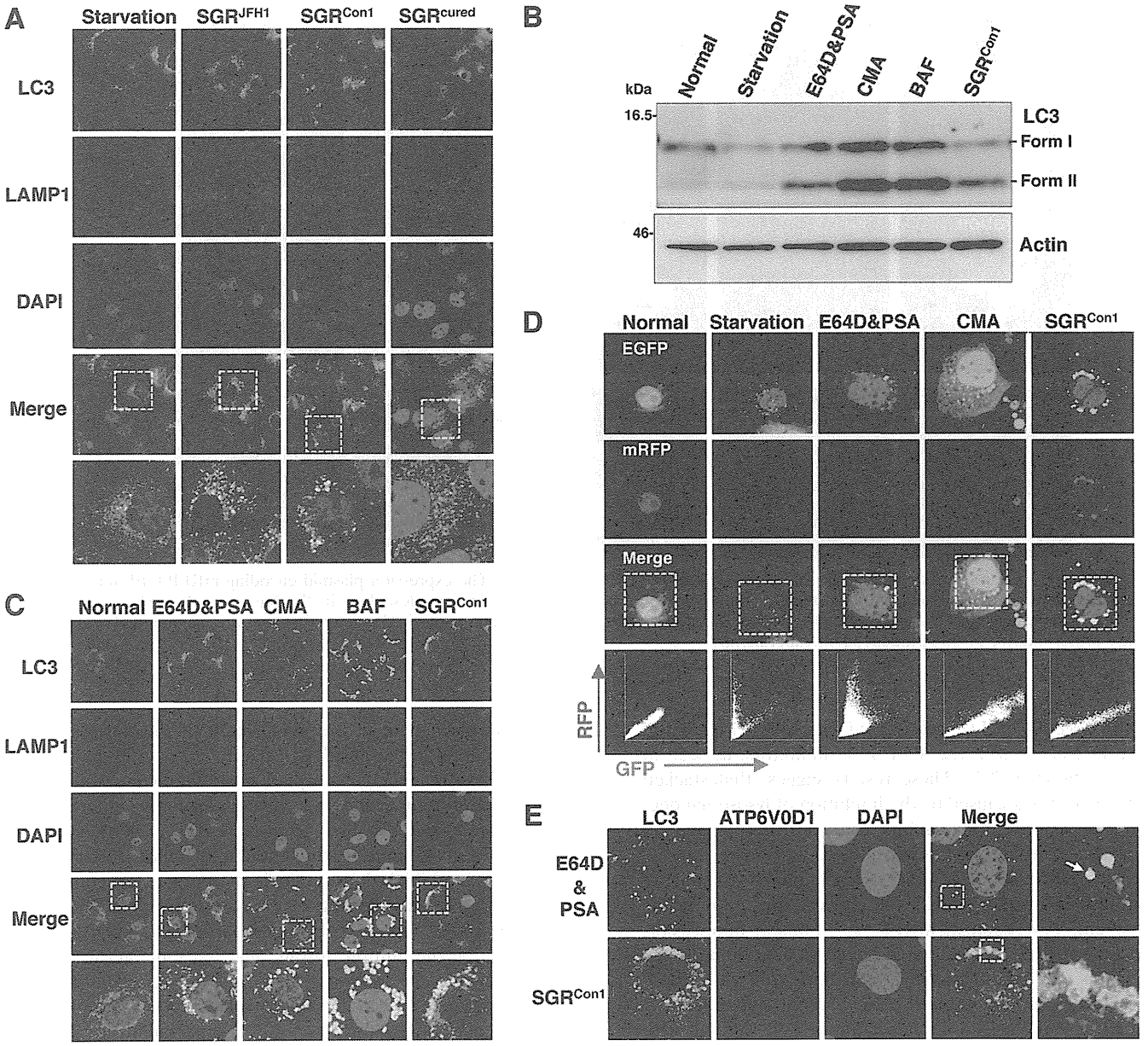

FIG. 3. Inhibition of autophagy maturation in HCV replicon cells. (A) After nuclear staining with DAPI, starved Huh7 cells, replicon cells, and SGR^{cured} cells were stained with rabbit polyclonal anti-LC3 and mouse monoclonal anti-LAMP1 antibodies followed by Alexa Fluor 488- and 594-conjugated secondary antibodies, respectively, and examined by confocal microscopy. The boxed regions in the merged images are magnified. (B and C) Huh7 cells were treated with 20 μM protease inhibitors (E64D and PSA) or a 20 nM concentration of a V-ATPase inhibitor (CMA or BAF) for 6 h. (B) Cell lysates were subjected to immunoblotting using antibodies against LC3 and β-actin. (C) Intracellular localization of LAMP1 and LC3 was determined by confocal microscopy after staining with DAPI and appropriate antibodies. The boxed areas in the merged images are magnified. (D) Tandem fluorescence-tagged LC3 assay. The expression plasmid encoding mRFP-GFP-tandem-tagged LC3 was transfected into naïve and starved Huh7 cells or into the SGR^{Con1} cells treated with the indicated inhibitors at 36 h posttransfection. The resulting cells were fixed at 42 h posttransfection, and the relative GFP and RFP signals were determined by confocal microscopy. The fluorescent values in the boxes of the merged images were determined and shown as dot plots in the bottom column of the grid, in which the *x* and *y* axes indicate the signals of GFP and RFP, respectively. (E) Huh7 cells treated with E64D and PSA and the SGR^{Con1} cells were stained with DAPI and then with rabbit polyclonal anti-LC3 and mouse monoclonal anti-ATP6V0D1 antibodies followed by Alexa Fluor 488- and 594-conjugated secondary antibodies, respectively. The boxed regions in the merged images are magnified. A white arrow indicates colocalization of LC3 and ATP6V0D1. The data shown are representative of three independent experiments.

drolases in the vesicle (2). Next, to determine the possibility of a deficiency in the acidification of the autolysosome on the autophagic dysfunction in the Con1 replicon cells, Huh7 cells were treated with the protease inhibitors E64D and pepstatin A (PSA) or with each of the V-ATPase inhibitors concanamycin A (CMA) and bafilomycin A1 (BAF). The amount of LC3-II was significantly increased in Huh7 cells treated with the inhibitors just as in the SGR^{Con1} cells (Fig. 3B). Further-

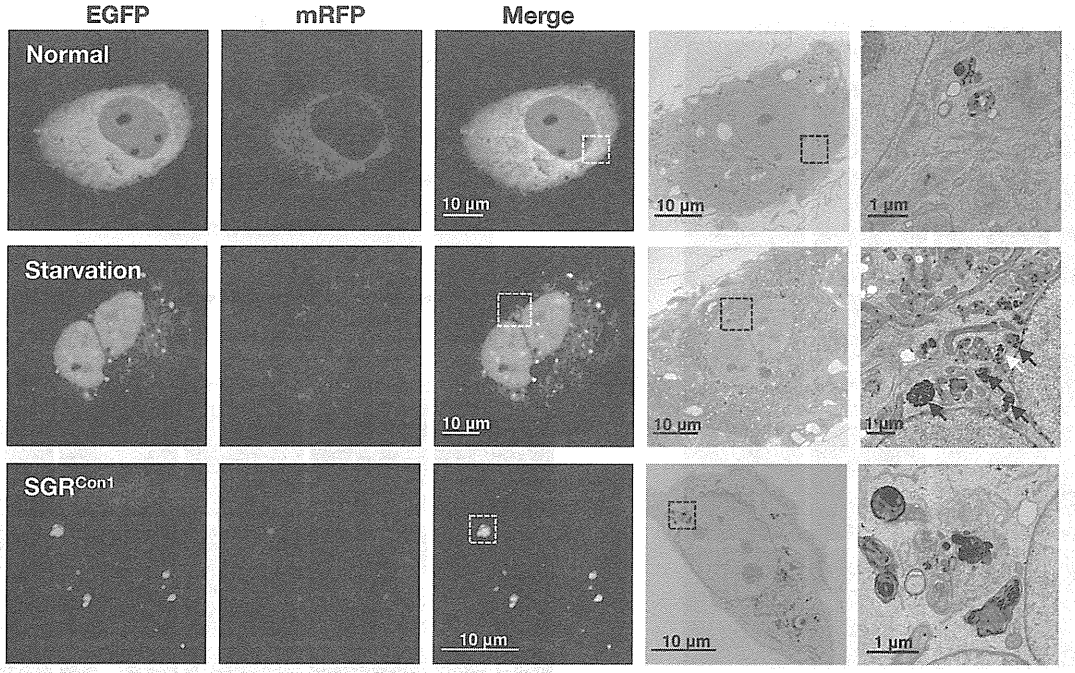

FIG. 4. Correlative fluorescence microscopy-electron microscopy (FM-EM) analysis. The expression plasmid encoding mRFP-GFP-tandem-tagged LC3 was transfected into naïve and starved Huh7 cells or into the SGR^{Con1} cells as described in the legend to Fig. 3D, and the mRFP-GFP-tandem-tagged LC3 signals were observed at 36 h posttransfection. The boxed regions in the merged images are magnified. The data shown are representative of three independent experiments.

more, the large foci of LC3 colocalized with LAMP1 appeared in the cells treated with the V-ATPase inhibitors, as seen in SGR^{Con1} cells (Fig. 3C). These results suggest that stacked autophagosome flux caused by the inhibition of lysosomal degradation or acidification exhibits characteristics similar to those observed in the Con1 replicon cells.

Since the fluorescence of GFP but not that of monomeric red fluorescent protein (mRFP) disappears under the acidic environment, expression of mRFP-GFP tandem fluorescent-tagged LC3 (tfLC3) is capable of being used to monitor the acidic status of the autolysosome (24). Both GFP and mRFP fluorescent signals were unfused, some of them accumulated as small foci in Huh7 cells after starvation or by treatment with the protease inhibitors, and half of the foci of mRFP were not colocalized with those of GFP (Fig. 3D), indicating that half of the foci are in an acidic state due to maturation into an autolysosome after fusion with a lysosome. On the other hand, the large foci of GFP and mRFP were completely colocalized in Huh7 cells treated with CMA or in the SGR^{Con1} cells. These results suggest that the large foci of LC3 in the SGR^{Con1} cells are not under acidic conditions. Recently, it was shown that the lack of lysosomal acidification in human genetic disorders due to dysfunction in assembly/sorting of V-ATPase induces incomplete autophagy similar to that observed in SGR^{Con1} cells (31, 45). Therefore, to explore the reason for the lack of acidification of the autolysosome in the SGR^{Con1} cells, we examined the subcellular localization of ATP6V0D1, a subunit of the integral membrane V_0 complex of V-ATPase. Colocalization of ATP6V0D1 with large foci of LC3 was observed in Huh7 cells treated with the protease inhibitors but not in SGR^{Con1} cells (Fig. 3E), suggesting that dislocation of V-ATPase may participate in the impairment of the autolysosomal acidification in the SGR^{Con1} cells.

We further examined the morphological characteristics of the LC3-positive compartments by using correlative fluorescence microscopy-electron microscopy (FM-EM) (Fig. 4). The starved Huh7 cells exhibited a small double-membrane vesicle (white arrow) and high-density single-membrane structures (black arrows) in close proximity to the correlative position of the GFP- and mRFP-positive LC3 compartments, which are considered to be the autophagosome and lysosome/autolysosome, respectively. In contrast, many high-density membranous structures were detected in the correlative position of the large GFP- and mRFP-positive LC3 compartment in the SGR^{Con1} cells, which is well consistent with the observation in the time-lapse imaging in which small foci of LC3 headed toward and assembled with the large LC3-positive compartment (see movies in the supplemental material). These results suggest that the formation of large aggregates with aberrant inner structures in the SGR^{Con1} cells may impair maturation of the autolysosome through the interference of further fusion with functional lysosomes for the degradation.

The secretion of immature cathepsin B is enhanced in the replicon cell of strain Con1. Lysosomal acidification is required for the cleavage of cathepsins for activation, and cathepsin B (CTSB) is processed under acidic conditions (13). Although a marginal decrease of CTSB was detected in the whole lysates of the SGR^{Con1} cells, a significant reduction in the expression of both unprocessed (pro-CTSB) and matured CTSB was observed in the lysosomal fractions of the SGR^{Con1} cells compared with those of the naïve Huh7 and the SGR^{cured} cells (Fig. 5A). LAMP1 was concentrated at a similar level in

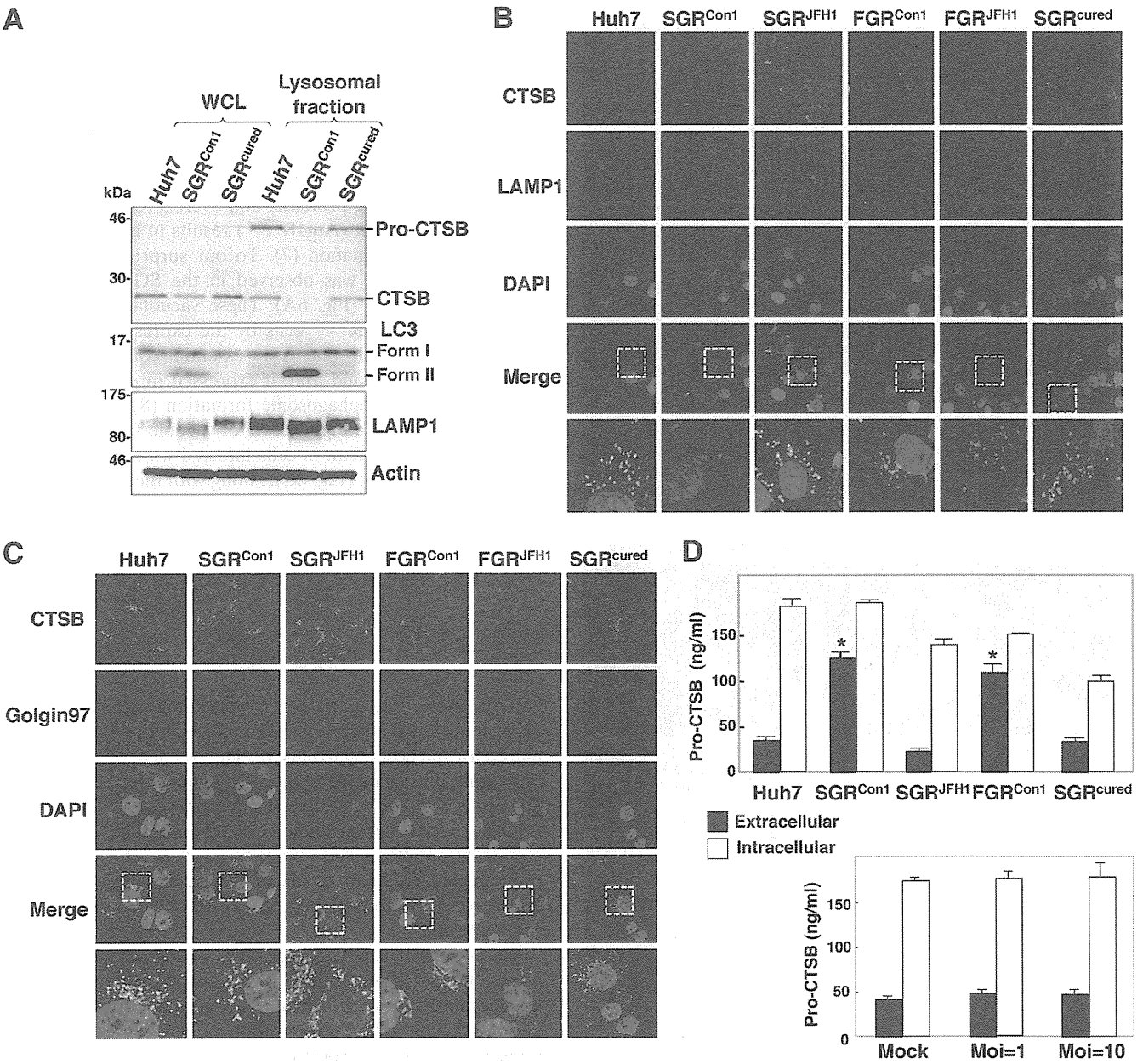

FIG. 5. Enhanced secretion of pro-CTSB in the HCV replicon cells. (A) The whole-cell lysate (WCL) and lysosomal fraction prepared from Huh7, SGR^{Con1}, and SGR^{cured} cells were subjected to immunoblotting. (B and C) Huh7 cells, HCV replicon cells, and SGR^{cured} cells were stained with DAPI, rabbit polyclonal anti-CTSB antibody, and mouse anti-LAMP1 (B) or anti-Golgin97 (C) antibody. The boxed areas in the merged images are magnified. (D) Expression of pro-cathepsin B in the culture supernatants (black bars) and cell lysates (white bars) of the Huh7, SGR^{Con1}, SGR^{JFH1}, FGR^{Con1}, and SGR^{cured} cells and the SGR^{cured} cells infected with HCVcc at a multiplicity of infection (Moi) of 1 or 10 and incubated for 72 h was determined by enzyme-linked immunosorbent assay (ELISA). The error bars indicate standard deviations. The asterisks indicate significant differences ($P < 0.01$) versus the control value. The data shown are representative of three independent experiments.

the lysosomal fractions of the cells, whereas LC-II was detected in the fractions of the SGR^{Con1} cells but not in those of Huh7 and the SGR^{cured} cells, suggesting that autophagosomes and/or autolysosomes in the SGR^{Con1} cells are fractionated in the lysosomal fraction. Colocalization of CTSB with LAMP1 was observed in the naïve Huh7 cells, in the SGR^{cured} cells, and in the replicon cells harboring a sub- or a full genomic RNA of strain JFH1 (SGR^{JFH1} and FGR^{JFH1}, respectively) but not in those of strain Con1 (SGR^{Con1} and FGR^{Con1}) (Fig. 5B). On the other hand, CTSB was colocalized with Golgin97, a marker for the Golgi apparatus, in the SGR^{Con1} and FGR^{Con1} cells but not in other cells (Fig. 5C). Since previous reports suggested that the alkalization in the lysosome triggers secretion of the unprocessed lysosomal enzymes (19, 41), we next determined the secretion of pro-CTSB in the replicon cells. Secretion of the pro-CTSB was significantly enhanced in the replicon cells of strain Con1 but not in those of strain JFH1 and naïve and cured cells (Fig. 5D, top). Furthermore, secretion of pro-CTSB

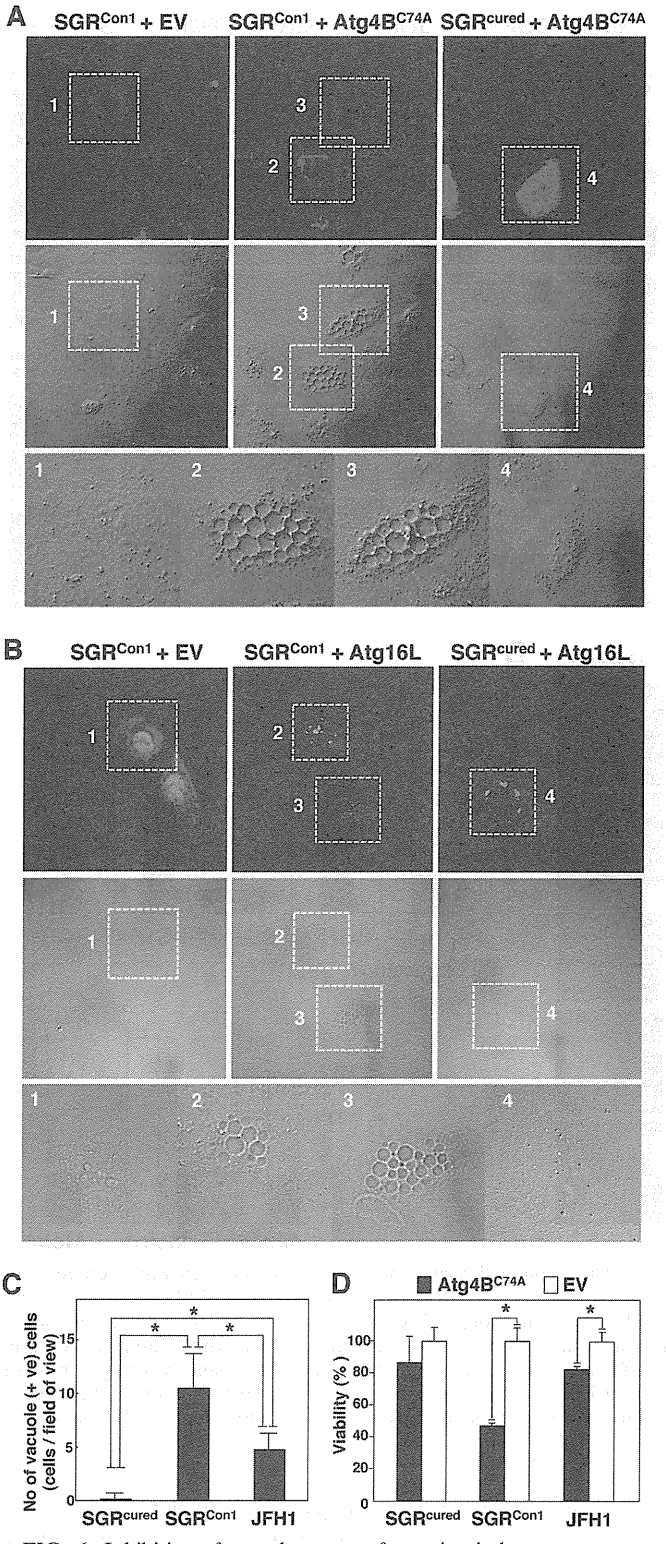

FIG. 6. Inhibition of autophagosome formation induces severe cytoplasmic vacuolations leading to cell death in the HCV replicon cells. (A) SGR^{Con1} and SGR^{cured} cells transfected with pStrawberry-$Atg4B^{C74A}$ or empty vector pStrawberry (EV) were fixed at 48 h posttransfection and examined by fluorescence microscopy. The boxed areas in the phase-contrast images are magnified. (B) SGR^{Con1} and SGR^{cured} cells transfected with pEGFP-Atg16L or EV were examined by fluorescence microscopy at 48 h posttransfection. The boxed areas in the phase-contrast images are magnified. (C) SGR^{cured}, SGR^{Con1}, and SGR^{cured} cells infected with JFH1 virus were transfected with pStrawberry-$Atg4B^{C74A}$, and the number of vacuole-positive cells in each of nine fields of view was counted at 48 h posttransfection. (D) SGR^{cured}, SGR^{Con1}, and SGR^{cured} cells infected with JFH1 virus were transfected with pStrawberry-$Atg4B^{C74A}$ (black bars) or EV (white bars), and cell viability was determined at 6 days posttransfection by using CellTiter-Glo (Promega) according to the manufacturer's protocol. The asterisks indicate significant differences ($P < 0.05$) versus the control value. The data shown are representative of three independent experiments.

was not observed in the cured cells infected with HCVcc, an infectious HCV strain derived from strain JFH1 (Fig. 5D, bottom). Collectively, these results suggest that the dysfunction of lysosomal acidification contributes to the impairment of autophagy in the HCV replicon cells of strain Con1.

Autophagy induced in cells replicating HCV is required for cell survival. Finally, we examined the pathological significance of autophagy during HCV replication. Atg4B is known as an LC3-processing protease, and overexpression of its protease-inactive mutant ($Atg4B^{C74A}$) results in inhibition of the autophagosome formation (7). To our surprise, severe cytoplasmic vacuolation was observed in the SGR^{Con1} cells expressing $Atg4B^{C74A}$ (Fig. 6A). These vacuolations were also observed in the SGR^{Con1} cells by the expression of Atg16L (Fig. 6B), a molecule that is an essential component of the autophagy complex and that, if expressed in excess amounts, can disrupt the autophagosome formation (8). Expression of $Atg4B^{C74A}$ induced a higher level of vacuole formation in the Con1 replicon cells than in cells infected with JFH1 virus but not in the cured cells (Fig. 6C). Along with these vacuolations, cell viability was significantly decreased by the expression of $Atg4B^{C74A}$ in SGR^{Con1} cells and slightly in JFH1 virus-infected cells (Fig. 6D). These results suggest that autophagy induced by the RNA replication of HCV is required for host cell survival.

DISCUSSION

In the present study, we demonstrated that two genotypes of HCV induce autophagy, whereas intact autophagy flux is required for the host cell to survive. The cell death characterized by cytoplasmic vacuolation that was induced in the HCV replicon cells by the inhibition of the autophagosome formation is similar to type III programmed cell death, which is distinguishable from apoptosis and autophagic cell death (4). Type III programmed cell death has been observed in the neurodegenerative diseases caused by the deposit of cytotoxic protein aggregates (15).

We previously reported that HCV hijacks chaperone complexes, which regulates quality control of proteins into the membranous web for circumventing unfolded protein response during efficient genome replication (53); in other words, the replication of HCV exacerbates the generation of proteins associated with cytotoxicity. In the experiments using a chimpanzee model, HCV of genotype 1 was successfully used to reproduce acute and chronic hepatitis similar to that in the human patients (3, 57), and transgenic mice expressing viral proteins of HCV of genotype 1b have been shown to develop

Sjögren syndrome, insulin resistance, hepatic steatosis, and hepatocellular carcinoma (27, 28). In contrast, HCVcc, based on the genotype 2a strain JFH1 isolated from a patient with fulminant hepatitis C (33, 56), was unable to establish chronic infection in chimpanzees (56) or to induce cell damage and inflammation in chimeric mice xenotransplanted with human hepatocytes (17). These results imply that the onset of HCV pathogenesis could be dependent not only upon an amount but also on a property of deposited proteins, and they might explain the aggravated vacuolations under the inhibition of autophagosome formation in strain Con1 compared to that in strain JFH1. Interestingly, the overexpression of $Atg4B^{C74A}$ or Atg16L causes eccentric cell death in the Con1 replicon cells in which autophagy flux is already disturbed. Thus, we speculated that the quarantine of undefined abnormalities endowed with high cytotoxicity by the engulfing of the autophagic membrane might be sufficient for the amelioration of HCV-induced degeneration. The autophagosomal dysfunction observed in the Con1 replicon cells may suggest that a replicant of strain Con1 was more sensitive to the lysosomal vacuolation than that of strain JFH1. Because a limitation of our study was that we were unable to use infectious HCV of other strains, it is still unclear whether the autophagic degradation can be impaired only in the replicon of HCV strain Con1 or genotype 1.

We also demonstrated that HCV replication of strain Con1 but not that of strain JFH1 facilitates the secretion of pro-CTSB. It has been well established that the secretion of pro-CTSB is enhanced in several types of tumors (26, 50). The secretion of CTSB, like the secretion of matrix metalloproteases, is a marker of the progression of the proteolytic degradation of the extracellular matrix, which plays an important part in cancer invasion and metastasis. Since infection with HCV of genotype 1 is clinically considered a risk factor for the development of hepatocellular carcinoma (14, 51), the enhanced secretion of pro-CTSB by the replication of genotype 1 strains might synergistically promote infiltration of hepatocellular carcinoma.

As shown elsewhere (see movies in the supplemental material), although most degradations of the autophagosome were impaired due to a dislocalization of a V-ATPase subunit, some autophagic degradation was achieved in the SGR^{Con1} cells similar to that in the starved Huh7 cells. Moreover, the stagnated autophagy flux was rescued by the treatment of alpha interferon accompanied by elimination of HCV (Fig. 1C and D). Interestingly, we observed neither a significant impairment of lysosomal degradation nor the intracellular activity of cathepsins in the replicon cells of HCV strain Con1 (data not shown). Therefore, there might be a specific dysfunction within the autolysosome during the replication of HCV strain Con1. Detailed studies are needed to elucidate how HCV strain Con1 disturbs the sorting of V-ATPase.

A close relationship between autophagy and the immune system has been gradually unveiled (47). Autophagy assists not only in the direct elimination of pathogens by hydrolytic degradation but also in antigen processing in antigen-presenting cells such as macrophage and dendritic cells (DC) for presentation by major histocompatibility complex (MHC) I and II (11). Moreover, autophagy plays important roles in T lymphocyte homeostasis (44). As such, in some instances, interruptions of autophagy can allow microorganisms to escape from the host immune system. Indeed, the immune response against herpes simplex virus was suppressed by blocking the autophagy (6). With regard to HCV, functionally impaired DC dysfunctions marked by poor DC maturation, impaired antigen presentation, and attenuated cytokine production have been reported in tissue culture models and chronic hepatitis C patients (1, 22, 46). In addition, reduction of cell surface expression of MHC-I in HCV genotype 1b replicon cells has been reported (55). We confirmed that levels of cell surface expression of MHC-I in the replicon cells of genotype 1b, but not of genotype 2a, were reduced in comparison with those in the cured cells (data not shown). Hence it might be feasible to speculate that the replication of HCV RNA of genotype 1 induces an incomplete autophagy for attenuating antigen presentation to establish persistent infection. In contrast, autophagy is known to serve as a negative regulator of innate immunity (21, 54). A recent report demonstrated that autophagy induced by infection with strain JFH1 or dengue virus attenuates innate immunity to promote viral replication (23), indicating that an HCV genotype 2a strain may facilitate autophagy to evade innate immunity.

In this study, we demonstrated that HCV utilizes autophagy to circumvent the cell death induced by vacuole formation for its survival. This unique strategy of HCV propagation may provide new clues to the virus-host interaction and, ultimately, to the pathogenesis of infection by various genotypes of HCV.

ACKNOWLEDGMENTS

We thank H. Murase and M. Tomiyama for their secretarial work. We also thank R. Bartenschlager and T. Wakita for providing cell lines and plasmids.

This work was supported in part by grants-in-aid from the Ministry of Health, Labor, and Welfare (Research on Hepatitis), the Ministry of Education, Culture, Sports, Science, and Technology, and the Osaka University Global Center of Excellence Program.

REFERENCES

1. **Auffermann-Gretzinger, S., E. B. Keeffe, and S. Levy.** 2001. Impaired dendritic cell maturation in patients with chronic, but not resolved, hepatitis C virus infection. Blood **97:**3171–3176.
2. **Beyenbach, K. W., and H. Wieczorek.** 2006. The V-type H+ ATPase: molecular structure and function, physiological roles and regulation. J. Exp. Biol. **209:**577–589.
3. **Bradley, D. W.** 2000. Studies of non-A, non-B hepatitis and characterization of the hepatitis C virus in chimpanzees. Curr. Top. Microbiol. Immunol. **242:**1–23.
4. **Clarke, P. G.** 1990. Developmental cell death: morphological diversity and multiple mechanisms. Anat. Embryol. (Berl.) **181:**195–213.
5. **Dreux, M., P. Gastaminza, S. F. Wieland, and F. V. Chisari.** 2009. The autophagy machinery is required to initiate hepatitis C virus replication. Proc. Natl. Acad. Sci. U. S. A. **106:**14046–14051.
6. **English, L., et al.** 2009. Autophagy enhances the presentation of endogenous viral antigens on MHC class I molecules during HSV-1 infection. Nat. Immunol. **10:**480–487.
7. **Fujita, N., et al.** 2008. An Atg4B mutant hampers the lipidation of LC3 paralogues and causes defects in autophagosome closure. Mol. Biol. Cell **19:**4651–4659.
8. **Fujita, N., et al.** 2008. The Atg16L complex specifies the site of LC3 lipidation for membrane biogenesis in autophagy. Mol. Biol. Cell **19:**2092–2100.
9. **Fujitani, Y., C. Ebato, T. Uchida, R. Kawamori, and H. Watada.** 2009. β-cell autophagy: a novel mechanism regulating β-cell function and mass: lessons from β-cell-specific Atg7-deficient mice. Islets **1:**151–153.
10. **Gannage, M., et al.** 2009. Matrix protein 2 of influenza A virus blocks autophagosome fusion with lysosomes. Cell Host Microbe **6:**367–380.
11. **Gannage, M., and C. Munz.** 2009. Autophagy in MHC class II presentation of endogenous antigens. Curr. Top. Microbiol. Immunol. **335:**123–140.
12. **Hara, T., et al.** 2006. Suppression of basal autophagy in neural cells causes neurodegenerative disease in mice. Nature **441:**885–889.
13. **Hasilik, A.** 1992. The early and late processing of lysosomal enzymes: proteolysis and compartmentation. Experientia **48:**130–151.

14. **Hatzakis, A., et al.** 1996. Hepatitis C virus 1b is the dominant genotype in HCV-related carcinogenesis: a case-control study. Int. J. Cancer **68:**51–53.
15. **Hirabayashi, M., et al.** 2001. VCP/p97 in abnormal protein aggregates, cytoplasmic vacuoles, and cell death, phenotypes relevant to neurodegeneration. Cell Death Differ. **8:**977–984.
16. **Hiraga, N., et al.** 2011. Rapid emergence of telaprevir resistant hepatitis C virus strain from wildtype clone in vivo. Hepatology (Baltimore, Md.) **54:** 781–788.
17. **Hiraga, N., et al.** 2007. Infection of human hepatocyte chimeric mouse with genetically engineered hepatitis C virus and its susceptibility to interferon. FEBS Lett. **581:**1983–1987.
18. **Ichimura, Y., E. Kominami, K. Tanaka, and M. Komatsu.** 2008. Selective turnover of p62/A170/SQSTM1 by autophagy. Autophagy **4:**1063–1066.
19. **Isidoro, C., et al.** 1995. Altered intracellular processing and enhanced secretion of procathepsin D in a highly deviated rat hepatoma. Int. J. Cancer **60:**61–64.
20. **Jacobson, I. M., P. Cacoub, L. Dal Maso, S. A. Harrison, and Z. M. Younossi.** 2010. Manifestations of chronic hepatitis C virus infection beyond the liver. Clin. Gastroenterol. Hepatol. **8:**1017–1029.
21. **Jounai, N., et al.** 2007. The Atg5 Atg12 conjugate associates with innate antiviral immune responses. Proc. Natl. Acad. Sci. U. S. A. **104:**14050–14055.
22. **Kanto, T., et al.** 1999. Impaired allostimulatory capacity of peripheral blood dendritic cells recovered from hepatitis C virus-infected individuals. J. Immunol. **162:**5584–5591.
23. **Ke, P. Y., and S. S. Chen.** 2011. Activation of the unfolded protein response and autophagy after hepatitis C virus infection suppresses innate antiviral immunity in vitro. J. Clin. Invest. **121:**37–56.
24. **Kimura, S., N. Fujita, T. Noda, and T. Yoshimori.** 2009. Monitoring autophagy in mammalian cultured cells through the dynamics of LC3. Methods Enzymol. **452:**1–12.
25. **Kiyosawa, K., et al.** 1990. Interrelationship of blood transfusion, non-A, non-B hepatitis and hepatocellular carcinoma: analysis by detection of antibody to hepatitis C virus. Hepatology **12:**671–675.
26. **Koblinski, J. E., et al.** 2002. Interaction of human breast fibroblasts with collagen I increases secretion of procathepsin B. J. Biol. Chem. **277:**32220–32227.
27. **Koike, K., et al.** 1997. Sialadenitis histologically resembling Sjogren syndrome in mice transgenic for hepatitis C virus envelope genes. Proc. Natl. Acad. Sci. U. S. A. **94:**233–236.
28. **Koike, K., T. Tsutsumi, H. Yotsuyanagi, and K. Moriya.** 2010. Lipid metabolism and liver disease in hepatitis C viral infection. Oncology **78**(Suppl. 1)**:**24–30.
29. **Komatsu, M., et al.** 2006. Loss of autophagy in the central nervous system causes neurodegeneration in mice. Nature **441:**880–884.
30. **Komatsu, M., et al.** 2007. Homeostatic levels of p62 control cytoplasmic inclusion body formation in autophagy-deficient mice. Cell **131:**1149–1163.
31. **Lee, J. H., et al.** 2010. Lysosomal proteolysis and autophagy require presenilin 1 and are disrupted by Alzheimer-related PS1 mutations. Cell **141:** 1146–1158.
32. **Levine, B., and G. Kroemer.** 2008. Autophagy in the pathogenesis of disease. Cell **132:**27–42.
33. **Lindenbach, B. D., et al.** 2005. Complete replication of hepatitis C virus in cell culture. Science **309:**623–626.
34. **Lohmann, V., et al.** 1999. Replication of subgenomic hepatitis C virus RNAs in a hepatoma cell line. Science **285:**110–113.
35. **Manns, M. P., et al.** 2001. Peginterferon alfa-2b plus ribavirin compared with interferon alfa-2b plus ribavirin for initial treatment of chronic hepatitis C: a randomised trial. Lancet **358:**958–965.
36. **McHutchison, J. G., et al.** 2009. Telaprevir with peginterferon and ribavirin for chronic HCV genotype 1 infection. N. Engl. J. Med. **360:**1827–1838.
37. **Mizushima, N.** 2007. Autophagy: process and function. Genes Dev. **21:**2861–2873.
38. **Moradpour, D., F. Penin, and C. M. Rice.** 2007. Replication of hepatitis C virus. Nat. Rev. Microbiol. **5:**453–463.
39. **Moriishi, K., and Y. Matsuura.** 2007. Host factors involved in the replication of hepatitis C virus. Rev. Med. Virol. **17:**343–354.
40. **Moriishi, K., and Y. Matsuura.** 2003. Mechanisms of hepatitis C virus infection. Antivir. Chem. Chemother. **14:**285–297.
41. **Oda, K., Y. Nishimura, Y. Ikehara, and K. Kato.** 1991. Bafilomycin A1 inhibits the targeting of lysosomal acid hydrolases in cultured hepatocytes. Biochem. Biophys. Res. Commun. **178:**369–377.
42. **Orvedahl, A., et al.** 2007. HSV-1 ICP34.5 confers neurovirulence by targeting the Beclin 1 autophagy protein. Cell Host Microbe **1:**23–35.
43. **Poordad, F., et al.** 2011. Boceprevir for untreated chronic HCV genotype 1 infection. N. Engl. J. Med. **364:**1195–1206.
44. **Pua, H. H., I. Dzhagalov, M. Chuck, N. Mizushima, and Y. W. He.** 2007. A critical role for the autophagy gene Atg5 in T cell survival and proliferation. J. Exp. Med. **204:**25–31.
45. **Ramachandran, N., et al.** 2009. VMA21 deficiency causes an autophagic myopathy by compromising V-ATPase activity and lysosomal acidification. Cell **137:**235–246.
46. **Saito, K., et al.** 2008. Hepatitis C virus inhibits cell surface expression of HLA-DR, prevents dendritic cell maturation, and induces interleukin-10 production. J. Virol. **82:**3320–3328.
47. **Schmid, D., and C. Munz.** 2007. Innate and adaptive immunity through autophagy. Immunity **27:**11–21.
48. **Schutte, K., J. Bornschein, and P. Malfertheiner.** 2009. Hepatocellular carcinoma—epidemiological trends and risk factors. Dig. Dis. **27:**80–92.
49. **Sir, D., et al.** 2008. Induction of incomplete autophagic response by hepatitis C virus via the unfolded protein response. Hepatology **48:**1054–1061.
50. **Sloane, B. F., et al.** 2005. Cathepsin B and tumor proteolysis: contribution of the tumor microenvironment. Semin. Cancer Biol. **15:**149–157.
51. **Stankovic-Djordjevic, D., et al.** 2007. Hepatitis C virus genotypes and the development of hepatocellular carcinoma. J. Dig. Dis. **8:**42–47.
52. **Strader, D. B., T. Wright, D. L. Thomas, and L. B. Seeff.** 2004. Diagnosis, management, and treatment of hepatitis C. Hepatology **39:**1147–1171.
53. **Taguwa, S., et al.** 2009. Cochaperone activity of human butyrate-induced transcript 1 facilitates hepatitis C virus replication through an Hsp90-dependent pathway. J. Virol. **83:**10427–10436.
54. **Tal, M. C., et al.** 2009. Absence of autophagy results in reactive oxygen species-dependent amplification of RLR signaling. Proc. Natl. Acad. Sci. U. S. A. **106:**2770–2775.
55. **Tardif, K. D., and A. Siddiqui.** 2003. Cell surface expression of major histocompatibility complex class I molecules is reduced in hepatitis C virus subgenomic replicon-expressing cells. J. Virol. **77:**11644–11650.
56. **Wakita, T., et al.** 2005. Production of infectious hepatitis C virus in tissue culture from a cloned viral genome. Nat. Med. **11:**791–796.
57. **Walker, C. M.** 1997. Comparative features of hepatitis C virus infection in humans and chimpanzees. Springer Semin. Immunopathol. **19:**85–98.
58. **Wasley, A., and M. J. Alter.** 2000. Epidemiology of hepatitis C: geographic differences and temporal trends. Semin. Liver Dis. **20:**1–16.
59. **Wong, J., et al.** 2008. Autophagosome supports coxsackievirus B3 replication in host cells. J. Virol. **82:**9143–9153.
60. **Yoshimori, T., and T. Noda.** 2008. Toward unraveling membrane biogenesis in mammalian autophagy. Curr. Opin. Cell Biol. **20:**401–407.

Research Article

EASL EUROPEAN ASSOCIATION FOR THE STUDY OF THE LIVER | JOURNAL OF HEPATOLOGY

Altered composition of fatty acids exacerbates hepatotumorigenesis during activation of the phosphatidylinositol 3-kinase pathway

Yotaro Kudo[1], Yasuo Tanaka[1], Keisuke Tateishi[1,*], Keisuke Yamamoto[1], Shinzo Yamamoto[1], Dai Mohri[1], Yoshihiro Isomura[1], Motoko Seto[1], Hayato Nakagawa[1], Yoshinari Asaoka[1], Motohisa Tada[2], Miki Ohta[1], Hideaki Ijichi[1], Yoshihiro Hirata[1], Motoyuki Otsuka[1], Tsuneo Ikenoue[1], Shin Maeda[3], Shuichiro Shiina[1], Haruhiko Yoshida[1], Osamu Nakajima[4], Fumihiko Kanai[2], Masao Omata[5], Kazuhiko Koike[1]

[1]*Department of Gastroenterology, Graduate School of Medicine, The University of Tokyo, 7-3-1 Hongo, Bunkyo-ku, Tokyo 113-8655, Japan;* [2]*Department of Medicine and Clinical Oncology, Graduate School of Medicine, Chiba University, 1-8-1 Inohana, Chuo-ku, Chiba-shi, Chiba 260-8670, Japan;* [3]*Department of Gas troenterology, Yokohama City University, Graduate School of Medicine, 3-9 Fuku-ura, Kanazawa-ku, Yokohama 236-0004, Japan;* [4]*Research Laboratory for Molecular Genetics, Yamagata University, Yamagata 990-9585, Japan;* [5]*Yamanashi Prefectural Central Hospital, 1-1-1 Fujimi, Kofu-shi, Yamanashi 400-8506, Japan*

Background & Aims: Some clinical findings have suggested that systemic metabolic disorders accelerate *in vivo* tumor progression. Deregulation of the phosphatidylinositol 3-kinase (PI3K)/Akt pathway is implicated in both metabolic dysfunction and carcinogenesis in humans; however, it remains unknown whether the altered metabolic status caused by abnormal activation of the pathway is linked to the protumorigenic effect.

Methods: We established hepatocyte-specific *Pik3ca* transgenic (Tg) mice harboring N1068fs*4 mutation.

Results: The Tg mice exhibited hepatic steatosis and tumor development. PPARγ-dependent lipogenesis was accelerated in the Tg liver, and the abnormal profile of accumulated fatty acid (FA) composition was observed in the tumors of Tg livers. In addition, the Akt/mTOR pathway was highly activated in the tumors, and in turn, the expression of tumor suppressor genes including *Pten*, *Xpo4*, and *Dlc1* decreased. Interestingly, we found that the suppression of those genes and the enhanced *in vitro* colony formation were induced in the immortalized hepatocytes by the treatment with oleic acid (OA), which is one of the FAs that accumulated in tumors.

Conclusions: Our data suggest that the unusual FA accumulation has a possible role in promoting *in vivo* hepato-tumorigenesis under constitutive activation of the PI3K pathway. The *Pik3ca* Tg mice might help to elucidate molecular mechanisms by which metabolic dysfunction contributes to *in vivo* tumor progression.

Keywords: Hepatocellular carcinoma; Fatty acids; NAFLD; Tumor suppressor genes.

Received 3 October 2010; received in revised form 25 March 2011; accepted 27 March 2011; available online 19 May 2011

*Corresponding author. Tel.: +81 3 3815 5411x33070; fax: +81 3 3814 0021.

E-mail address: ktate-tky@umin.ac.jp (K. Tateishi).

Abbreviations: PI3K, phosphatidylinositol 3-kinase; Tg, transgenic; FA, fatty acid; OA, oleic acid; HCC, hepatocellular carcinoma; PTEN, phosphatase and tensin homolog deleted on chromosome 10; FBS, fetal bovine serum; Erk, extracellular signal-regulated kinase; WT, wild type; PA, palmitic acid; H&E, hematoxylin and eosin; NASH, non-alcoholic steatohepatitis.

Introduction

Accumulating clinical evidence suggests that systemic metabolic disorders including obesity and insulin resistance can affect or even promote *in vivo* tumor progression [1–4]. Some studies have outlined the impact of fat-enriched diets in the development of hepatocellular carcinoma (HCC) [5–7]. However, the mechanistic insights regarding metabolites or cellular signaling responsible for the development of HCC in altered metabolic states remain unknown.

The phosphatidylinositol 3-kinase (PI3K)/Akt signaling pathway is involved in various cellular processes including cell metabolism, growth, and survival [8,9]. The altered expression and mutation of PI3K/Akt-related signaling components have been detected in some human cancers [10]. In particular, the *PIK3CA* gene encoding p110α, which is a catalytic subunit of PI3K, has somatic mutations in some carcinomas [11]. Additionally, a mutation in its kinase domain has been reported in HCC and gastric cancer [12]. These findings indicate that deregulated PI3K activity plays certain roles in oncogenesis in humans [11,13]. PI3K signaling is antagonized by phosphatase and tensin homolog deleted on chromosome 10 (PTEN) phosphatase [14]. The expression of PTEN is decreased or absent in approximately half of HCC patients [15], and hepatocyte-specific *Pten* knockout

mice develop steatohepatitis and HCC [16]. These findings indicate that PTEN is a tumor suppressor in the liver [17]. Although recent reports have suggested unique functions of PTEN that are independent of the PI3K-Akt axis [18–20], it is unknown whether the phenotype in *Pten*-deficient mice is due to PI3K-dependent or PI3K-independent processes.

To address the pathological consequences caused by the abnormal activation of PI3K pathway *in vivo*, we generated liver-specific *Pik3ca* transgenic (Tg) mice. In this study, we proposed that abnormal fat composition, as observed in the *Pik3ca* Tg liver, is a mechanism by which metabolic deregulation is linked to *in vivo* tumor progression.

Materials and methods

Generation of Pik3ca Tg mice

The *Pik3ca* Tg mice were generated as described previously [21]. Briefly, Myc-tagged mouse *Pik3ca* cDNA (N1068fs*4) was cloned into the p2335A-1 vector (provided by Drs. Palmiter and Chisari) [22,23]. The microinjection was conducted by the Research Laboratory for Molecular Genetics, Yamagata University. Founder BDF1 mice (F0) were backcrossed with C57BL/6JJcl mice (CLEA Japan, Japan), and F5 mice were analyzed. The primers for genotyping were 5′-ATGGAACAGAAACTCATCTCT-3′ and 5′-GGGTGACACTTACGAAAAT-3′. All procedures involving animals were performed in accordance with protocols approved by the institutional committee for animal research at the University of Tokyo and complied with the Guide for the Care and Use of Laboratory Animals.

Cell cultures, viruses, and treatment with fatty acids

Lentiviral short hairpin RNA vectors were purchased from Open Biosystems (Huntsville, AL, USA). BNL-CL2 cells were infected with the virus according to the manufacturer's protocol and selected by puromycin. BNL-CL2 cells were incubated with either 50 μmol/L fatty acids or ethanol (mock) for 12 h in the absence of fetal bovine serum (FBS) in some experiments.

Antibodies and primers

The primers for quantitative RT-PCR are shown in Supplementary Table 1. Antibodies against phospho-Akt (Ser473 and Thr308), Akt, phospho-extracellular signal-regulated kinase (Erk) 1/2 (Thr202/Tyr204), Erk1/2, phospho-TSC2, phospho-S6K, TSC2, S6K, and SREBP1 were obtained from Cell Signaling Technology (Danvers, MA, USA). The anti-PTEN antibody was purchased from Neomarkers Inc. (Frement, CA, USA). The anti-TFIID antibody was purchased from Upstate Biotechnology Inc. (Lake Placid, NY, USA). For immunohistochemistry, the anti-phospho-Akt (Ser473) antibody and anti-Myc antibodies (Cell Signaling Technology) were used. The immunoblot data were quantified using Multi Gauge ver. 3.1 software (Fuji Film Corp., Tokyo, Japan).

Triacylglycerol content, serum alanine aminotransferase (ALT) levels, and FA composition

Triacylglycerols were extracted from the liver with chloroform–methanol (2:1, v/v), and the levels were determined by the GK-GPO method (Wako, Tokyo, Japan). Serum samples for ALT measurement were collected after a 16-h starvation (SRL, Tokyo, Japan). Fatty acids were extracted from frozen liver samples, and the composition was analyzed by gas chromatography (Kotobiken Medical Laboratories, Inc., Tokyo, Japan).

Glucose tolerance tests

Glucose was intraperitoneally injected into 8-week-old mice fasting for 16 h (1.5 mg of glucose/g body weight). Glucose concentration was measured using the FreeStyle FREEDOM Blood Glucose Monitoring System (Nipro, Tokyo, Japan) at 0, 15, 30, 60, 90, and 120 min after injection.

Oxidative stress evaluation

The measurement of hydrogen peroxide concentrations was performed by the Colorimetric Hydrogen Peroxide Kit (Assay Designs, Inc., Ann Arbor, MI, USA). Thiobarbituric acid reactive substances (TBARS) were measured by the TBARS Assay Kit (ZeptoMetrix, Buffalo, NY, USA).

Immunohistochemistry

Antigen retrieval on paraffin sections was performed by the acetylation method. Proteins were visualized using the standard 3,3′-diaminobenzidine protocol.

Soft agar assay

The lower layer of 0.5% agar in media was placed in a 35-mm dish. Cells (2.5×10^4) were suspended in the upper layer of 0.3% agar. Colonies (>25 μm in diameter) were counted after 14 days. Oleic acid (OA) (50 μmol/L) or ethanol was added to the upper layer in some experiments.

Statistics

All results are indicated as means ± SE. Statistics were performed by Student's *t*-test or ANOVA followed by Fisher's PLSD host-hoc test. *p*-Values <0.05 were considered statistically significant.

Results

Generation of hepatocyte-specific Pik3ca Tg mice

We established 2 independent lines of hepatocyte-specific Tg mice (*Pik3ca* Tg mice) harboring an "N1068fs*4" mutation in the kinase domain [12]. Myc-tagged mutant *Pik3ca* was designed to be expressed under the albumin promoter (Supplementary Fig. 1), and the liver-specific expression of the transgene was confirmed as shown in Fig. 1A. To assess the *in vivo* effect of the *Pik3ca* N1068fs*4 transgene, we analyzed the activity of molecules downstream of PIK3CA including Akt, TSC2, and S6K via immunoblotting. The phosphorylation of Akt, TSC2, and S6K was clearly increased both in the two lines of Tg livers, but not in the wild-type (WT) livers (Fig. 1B).

Constitutive activation of Pik3ca leads to fat accumulation in the liver

Both lines of *Pik3ca* Tg mice survived, and no difference in total body weight was observed between *Pik3ca* Tg and WT mice at 4 or 24 weeks of age (data not shown). The *Pik3ca* Tg2 mice exhibited better glucose tolerance than WT mice at 8 weeks (Supplementary Fig. 2). The ratio of liver weight to body weight was significantly increased in the *Pik3ca* Tg mice compared to that of WT mice (Fig. 2A). The livers of 4 week-old *Pik3ca* Tg mice appeared slightly enlarged and light-colored, and they exhibited obvious fatty changes by 24 weeks (Fig. 2B). The Tg livers contained a greater volume of triacylglycerol than WT (Fig. 2C). The results of Western blotting revealed that Tg2 mice exhibited a relatively low activation of Akt and S6K as compared to Tg1 (Fig. 1B); however, hepatic triacylglycerol levels were clearly increased in the two lines Tg mice (Fig. 2C). Indeed, even Tg2 mice demonstrated an obvious fatty change in their livers by 24 weeks (Fig. 2B and D). These findings indicated that the constitutive expression of the *Pik3ca* N1068fs*4 transgene has a potential to establish *in vivo* hepatic steatosis. In addition, we found

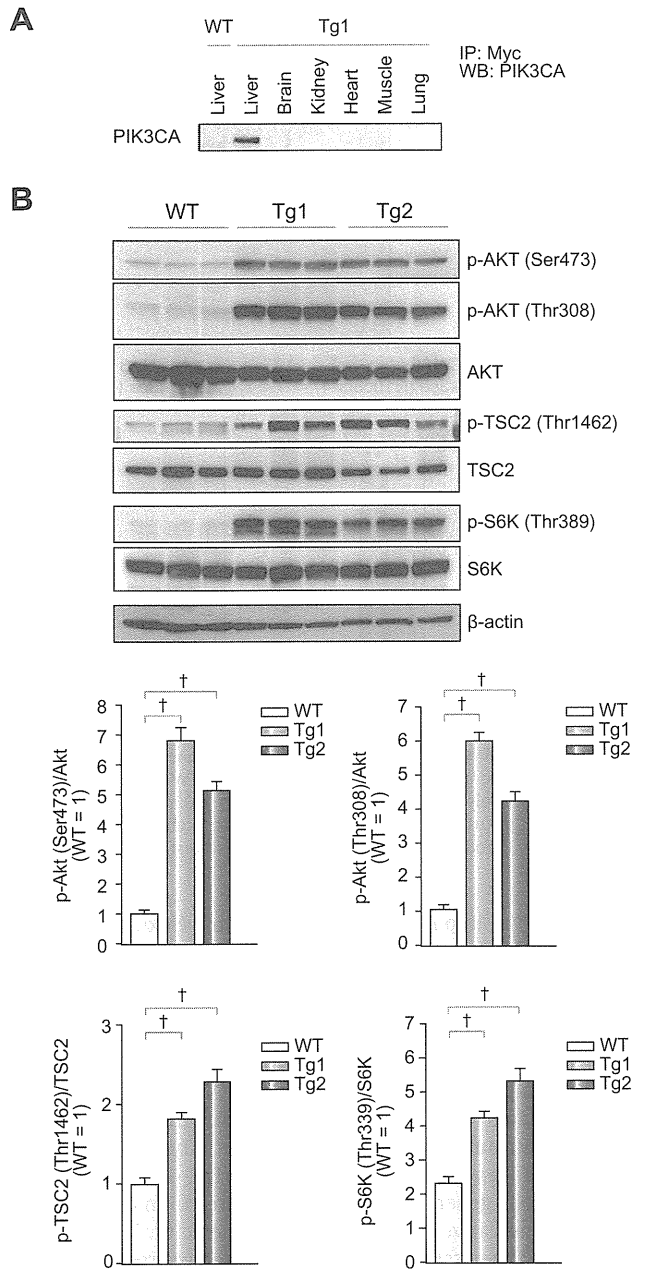

Fig. 1. Establishment of *Pik3ca* Tg mice. (A) Liver-specific expression of the mutant PIK3CA (N1068fs*4). (B) Immunoblots and quantification of the ratios of phosphorylated-Akt, TSC2, and S6K levels to total protein levels (†p <0.05, ANOVA; post hoc test with WT).

that ALT levels in the *Pik3ca* Tg mice were higher than those of WT mice (Fig. 2E), suggesting the coexistence of liver damage. Next, we examined how the *Pik3ca* Tg liver induced unusual lipid accumulation. Because lipogenesis is mainly mediated by two major transcription factors, PPARγ and SREBP1C [24,25], we measured their expression levels and their target genes in Tg2 mice livers and observed the upregulation of PPARγ and its target aP2 but not of SREBP1C or its target FASN (Fig. 2F). Given the previous finding that activated PI3K signaling can induce steatosis through PPARγ [26], we speculated that PPARγ-dependent lipogenesis is a process responsible for hepatic steatosis in Tg mice. This was supported by the finding that the nuclear accumulation of the active form of SREBP1c protein was not increased by *Pik3ca* (N1068fs*4) expression (Supplementary Fig. 3). To emphasize this notion, we investigated whether the *in vitro* overexpression of *Pik3ca* (N1068fs*4) induced lipid accumulation and the activation of PPARγ-dependent transcription. The *in vitro* overexpression of *Pik3ca* (N1068fs*4) increased the concentration of triacylglycerol in BNL-CL2 cells, immortalized normal hepatocytes derived from a BALB/c mouse [27] (Fig. 2G), and upregulated *aP2* expression (Fig. 2H). These data indicated that the overexpression of *Pik3ca* (N1068fs*4) directly contributes to the enhanced lipogenesis, at least via activating PPARγ-dependent transcription. Given the important role of mTOR in lipogenesis through PPARγ, there is a possibility that the activation of mTOR signaling (Fig. 1B) contributes to deregulated lipogenesis through PPARγ signaling in the *Pik3ca* Tg liver [26].

Tumor formation without inflammation in the Pik3ca Tg mice

Regardless of the marked fatty changes and suggested liver damage, *Pik3ca* Tg livers did not exhibit cellular infiltration or fibrotic change even at 52 weeks of age (Fig. 3A and B), which means the expression of the *Pik3ca* transgene is not sufficient for progression to steatohepatitis in the mouse liver. We found that the inflammatory cytokine IL-1α and Fas ligand were highly expressed in the *Pik3ca* Tg liver than WT (Supplementary Fig. 4). Given the previous findings that these factors can be responsible for liver damage [28,29], the abnormal upregulation of IL-1α and Fas ligand in Tg livers may explain a part of the mechanisms of liver damage, whereas the entire molecular process inducing them remains unknown. Notably, macroscopic hepatic tumors developed in 94% of Tg1 mice (30/32) and 100% of Tg2 mice (11/11) at 52 weeks of age (Fig. 3C, left). Most of the tumors were hepatocellular adenomas containing abundant lipid droplets (Fig. 3C, right). Some tumors had rough surfaces and irregular shapes with necrosis and hemorrhaging (Fig. 3D, left) and microscopically demonstrated characteristics of HCC such as enlarged and hyperchromatic nuclei and trabecular patterns (Fig. 3D, right). HCC tissues did not always exhibit lipid accumulation as shown in Fig. 3D. As the *Pik3ca* Tg mice aged, hepatic tumors became increased in number and size, whereas no WT littermates developed any tumors (Fig. 3E). These data clearly indicate that the *in vivo* constitutive expression of *Pik3ca* (N1068fs*4) leads to hepatic tumor development. To assess the functional activity of PIK3CA (N1068fs*4) for tumorigenesis, we examined the *in vitro* transforming ability using BNL-CL2 cells. Remarkably, *Pik3ca* (N1068fs*4) expression did not stimulate colony formation of BNL-CL2 cells (Supplementary Fig. 5). In addition, we analyzed the phosphorylation level of Akt by the *in vitro* overexpression of *Pik3ca* genes including wild type, H1047R, or N1068fs*4 in 293T cells. The overexpression of *Pik3ca* (H1047R) possessing *in vitro* transforming capacity [13] resulted in strong phosphorylation of Akt, as previously reported (Supplementary Fig. 6) [30]. Conversely, the overexpression of *Pik3ca* (wild type) without any transforming capacity [13] resulted in lower phosphorylation of Akt. The mutant PIK3CA (N1068fs*4) induced phosphorylation of Akt, but the level was comparable to that of wild type, and less than that of H1047R (Supplementary Fig. 6). These findings suggested that *Pik3ca* (N1068fs*4), as compared to H1047R, has less capacity for activating Akt and little

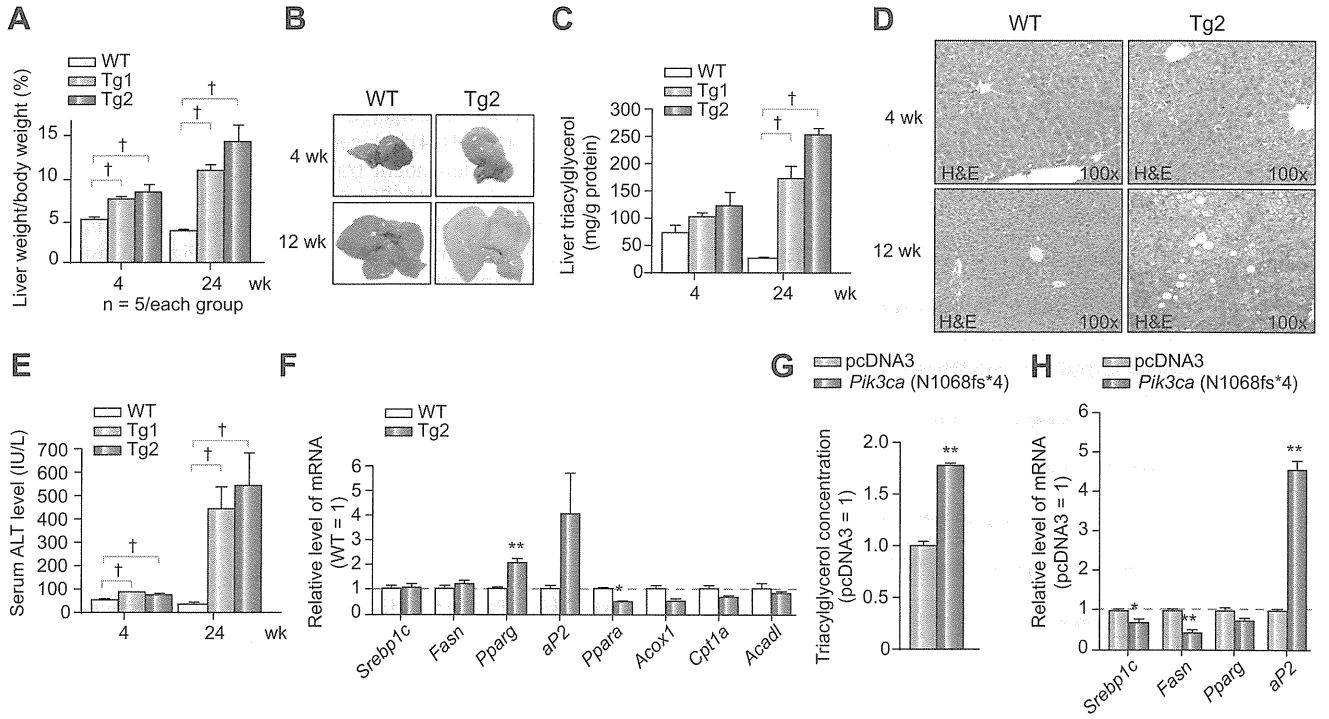

Fig. 2. Steatosis in the *Pik3ca* Tg liver. (A) Increased liver weight in *Pik3ca* Tg mice. (N = 5/group; †p <0.05, ANOVA; post hoc test with WT). (B) Representative liver images of WT and *Pik3ca* Tg mice. (C) High concentrations of intrahepatic triacylglycerol in the Tg mice (N >5/group; †p <0.05, ANOVA; post hoc test with WT). (D) H&E staining of livers from WT and *Pik3ca* Tg mice at 4 weeks (top) and 24 weeks (bottom) of age. (E) Higher serum ALT levels in the Tg mice (N = 5/group; †p <0.05, ANOVA; post hoc test with WT). (F) The expression of fat metabolism genes in the 4-week-old liver (N = 3–4/group; *p <0.05, **p <0.01, Student's t-test). (G) Cellular triacylglycerol levels and (H) the expression of lipogenesis-related genes in BNL-CL2 cells stably expressing *Pik3ca* (N1068fs*4) (N = 3/group; *p <0.05, **p <0.01, Student's t-test).

oncogenic activity in itself [13] and that there might be unknown factors promoting *in vivo* tumorigenesis in the *Pik3ca* Tg liver.

Downregulation of tumor suppressor genes in tumors derived from Pik3ca Tg livers

To further assess the related cellular signaling for tumorigenesis in the *Pik3ca* liver, we evaluated the activation of Akt, S6K, and Erk among the WT liver, non-tumor Tg liver, and tumor tissues from 52-week-old mice (Fig. 4A). Tumor tissues exhibited significantly enhanced activation of Akt compared to the Akt activation in non-tumor background or WT livers. We observed stronger phosphorylation of Akt in the non-tumor Tg liver than in WT livers, but the difference was not statistically significant as determined by ANOVA. Furthermore, the immunohistochemistry for phospho-Akt did not demonstrate clear differences between non-tumor livers and WT tissues. In contrast, the expression of *Myc-Pik3ca* was sustained in the non-tumor liver at 52 weeks (Supplementary Fig. 7). Those findings suggest the possibility that continuous activation of Akt induced by overexpressed *Pik3ca* is important for tumor formation in the Tg livers [31], whereas it remains unknown why Akt phosphorylation was attenuated in the non-tumor liver at 52 weeks despite the sustained expression of *Pik3ca* (Fig. 4A and Supplementary Fig. 7). In addition, the phosphorylation of S6K and Erk tended to be higher in Tg livers than in WT livers (Fig. 4A), but the difference became attenuated at 52 weeks compared to that at 4 weeks (Figs. 1B and 4A and Supplementary Fig. 8). These data do not exclude the possible role of these molecules in tumorigenesis in Tg livers but at least may emphasize the importance of Akt activation. Next, we examined the expression levels of genes involved in murine hepatotumorigenesis [32–34]. We observed decreased expression of four tumor suppressor genes, *Pten*, AT-rich interactive domain 5B (*Arid5b*), exportin 4 (*Xpo4*), and deleted in liver cancer 1 (*Dlc1*), in the tumor compared to the non-tumor background of *Pik3ca* Tg livers (Fig. 4B and Supplementary Fig. 9). PTEN protein levels were downregulated (Fig. 4C). To address whether the downregulation of *Pten* contributes to the tumorigenic activity in liver cells, we established *Pten*-depleted BNL-CL2 cells (Fig. 4D). *Pten*-depleted BNL-CL2 cells generated significantly more colonies in soft agar (Fig. 4E), indicative of enhanced tumorigenicity. These findings emphasize the possibility that the decreased expression of tumor suppressor genes has a certain role in tumorigenesis in the *Pik3ca* Tg liver. Importantly, the *in vitro* overexpression of mutant *Pik3ca* (N1068fs*4) only suppressed *Arid5b* expression but did not decrease the expression of *Pten*, *Xpo4*, or *Dlc1* in BNL-CL2 cells, indicating that certain additional mechanisms repressed their expression (Supplementary Fig. 10). Although several reports suggested a relationship between oxidative stress and hepatocarcinogenesis [35], the levels of hydrogen peroxide and lipid peroxidation were comparable between Tg and WT livers (Supplementary Fig. 11).

Tumors contain higher concentrations of OAs and palmitic acids (PAs) compared to the background tissues in the Pik3ca Tg liver

Recent intensive research has shed light into the significance of fatty acid (FA) as a potent biological stimulator of intracellular

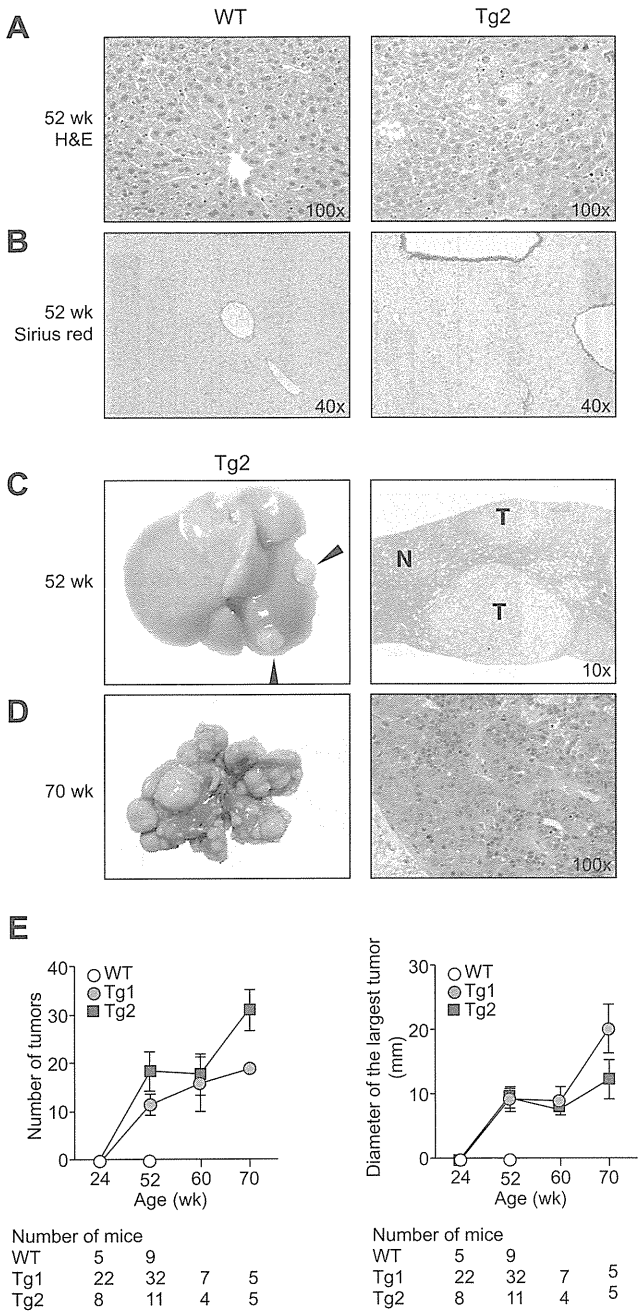

Fig. 3. Liver tumors in the *Pik3ca* Tg mice. (A) H&E and (B) Sirius red staining of livers at 52 weeks. (C) Macroscopic view (left) of the representative liver adenomas (arrowheads) at 52 weeks of age. H&E staining of an adenoma (T) and adjacent parenchyma (N) (right). (D) Tumors in *Pik3ca* Tg mice at 70 weeks (left). H&E staining of HCC (right). (E) The number (left) and size (right) of hepatic tumors. The number of mice examined is shown below the graphs.

signaling [36]. Interestingly, unsaturated FAs inhibit *Pten* expression via microRNA-21 in hepatoma [7,37,38], and the overexpression of a FA receptor (FFAR2) transformed the 3T3 fibroblasts [39], suggesting the possible relationship between FA and tumorigenesis. In the *Pik3ca* Tg liver, the tumor tissues contained higher concentrations of FAs than the non-tumor background tissues (Fig. 5A). The difference in total FA levels was largely due to the increase in levels of OA (C18:1n9) and PA (C16:0) in the tumors (Fig. 5B and C, Supplementary Fig. 12 and Table 2).

OA has the potential to repress the expression of tumor suppressors and enhance colony formation in vitro

To examine the possibility that either OA or PA downregulates the expression of tumor suppressors including *Pten*, we treated BNL-CL2 cells with OA or PA. OA, but not PA, repressed the expression of *Pten*, *Arid5b*, *Xpo4*, and *Dlc1* (Fig. 6A). Moreover, BNL-CL2 cells exposed to OA formed significantly more colonies in soft agar (Fig. 6B). These findings indicate that OA potentially enhances the in *vivo* tumorigenesis in the *Pik3ca* Tg liver. As an example, it is likely that decreased PTEN expression could enhance the Akt activation by the *Pik3ca* transgene in Tg-derived tumors (Fig. 1B).

Discussion

Hepatocyte-specific overexpression of *Pik3ca* (N1068fs*4) leads to steatosis and hepatic tumor formation. This mutation was originally isolated in human HCC and gastric cancers [12], but its functional analysis has never been reported. The *in vitro* overexpression of this mutant clearly induced Akt activation, but the level of activation was comparable with that of *Pik3ca* wild type and lower than that of the oncogenic H1047R mutant, suggesting that the *Pik3ca* Tg mice provide a model for studying effects of PIK3CA overexpression rather than a gain-of-function of PIK3CA. Furthermore, the N1068fs*4 mutation was not sufficient for cellular transformation *in vitro*, different from *Pik3ca* H1047R [40]. Considering results from a previous report suggesting the pivotal role of Akt activation in cell transformation by *PIK3CA* mutation [13], the activation level of Akt induced by *Pik3ca* (N1068fs*4) expression should not be sufficient for the cell-transforming process. These data indicated that the development of hepatic tumors in Tg mice might not be always a direct effect of *Pik3ca* (N1068fs*4) but instead promoted by other *in vivo* protumorigenic factors.

We focused on FA as an additional protumorigenic factor contributing to *in vivo* hepato-tumorigenesis in Tg mice, based on recent research on their oncogenic capacity [39]. Previous studies reported that OA inhibits *PTEN* expression via the upregulation of microRNA-21 through an mTOR/NF-κB-dependent mechanism [37,38] and also that exposure to OA increases tumor growth in xenografts [7]. Here, we demonstrated the correlation between OA accumulation and downregulation of other tumor suppressors, whereas the entire molecular mechanism remains to be elucidated. At least, there is a possibility that, in the Tg-derived tumors, OA accumulation enhanced the Akt activation by the *Pik3ca* transgene, which phosphorylates Akt less strongly than other oncogenic mutants *in vitro* (Fig. 1B, Supplementary Figs. 6 and 13).

Lipogenesis is mainly mediated by two major transcription factors, PPARγ and SREBP1C [24,25]. Hepatocyte-specific *Pten* KO mice exhibited increased expression of both PPARγ and SREBP1c in the liver, whereas only PPARγ was highly expressed in the *Pik3ca* Tg liver [16]. Our *in vitro* data suggested that the PI3K signaling is upstream of the activation of PPARγ in hepatocytes. A recent study shows that levels of *PPARγ* as well as *SREBP1c* mRNA are higher in the livers of patients with steatosis

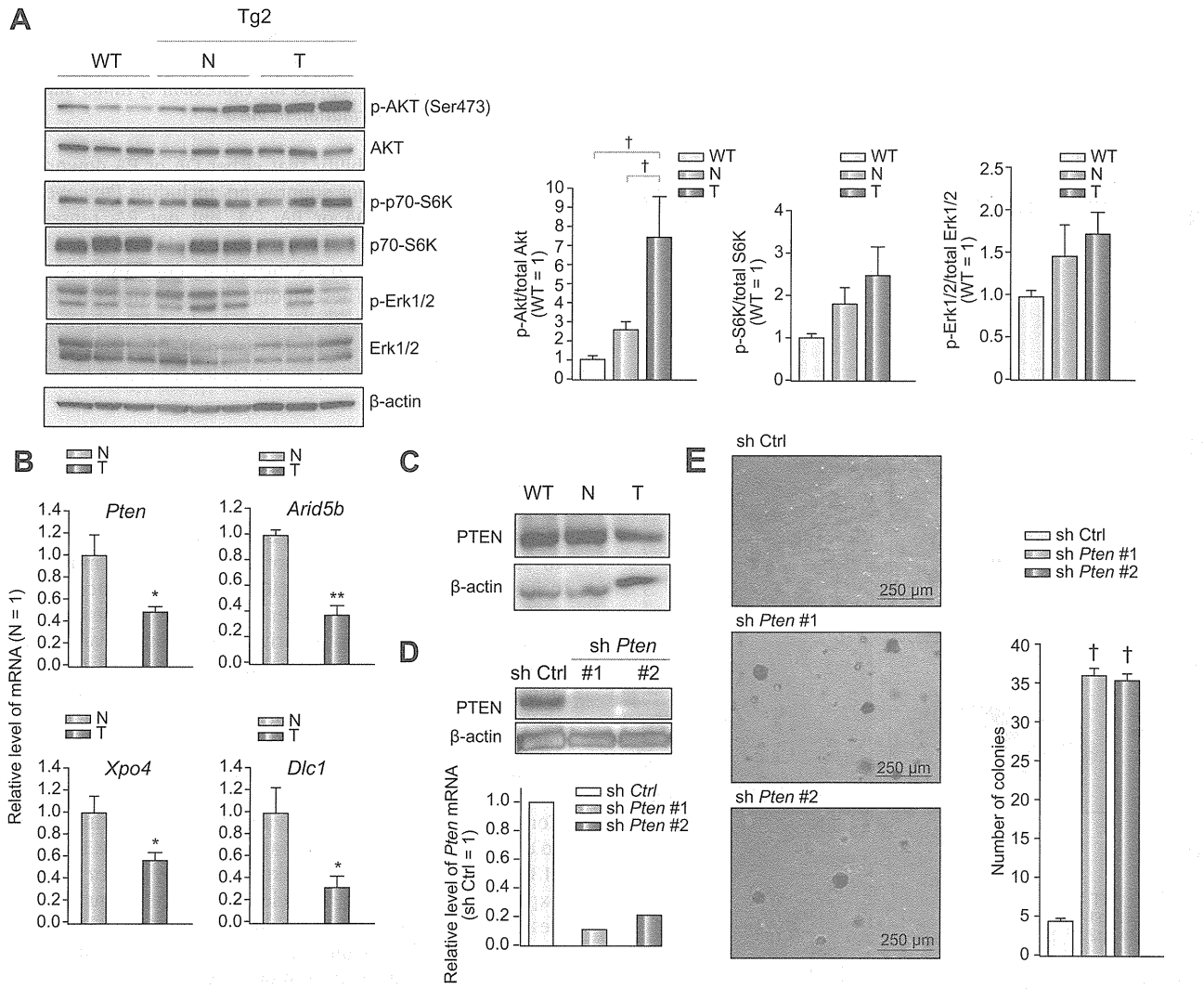

Fig. 4. *Pten* downregulation in the *Pik3ca* Tg liver. (A) Immunoblots and quantification of liver homogenates at 52 weeks ($^{\dagger}p$ <0.05, ANOVA; post hoc test with WT). (B) The decreased expression of *Pten*, *Arid5b*, *Xpo4*, and *Dlc1* mRNA in the *Pik3ca* Tg liver tumors (T) relative to their expression in background liver tissues (N) (N = 5/group; $^{*}p$ <0.05, $^{**}p$ <0.01, Student's *t*-test). (C) Representative images of immunoblots of liver tissues from the littermates at 52 weeks. (D) Knockdown of *Pten* in BNL-CL2 cells confirmed at the protein (top) and mRNA (bottom) levels. (E) Both lines of *Pten*-depleted BNL-CL2 cells (sh*Pten* #1 and #2) formed more colonies in soft agar (N = 3/group; $^{\dagger}p$ <0.05, ANOVA; post hoc test with control cells (shCtrl)).

or steatohepatitis, suggesting that the activity of PPARγ is implicated in the abnormal lipid accumulation in human livers [41] (Supplementary Fig. 13).

Unlike the hepatocyte-specific *Pten* KO mice [16], cellular infiltration and fibrosis were not observed in the *Pik3ca* Tg liver. One explanation is the possibility that *Pten* deficiency induces certain pathological mechanisms independently of PI3K-Akt activation, as previously reported for mammary tumorigenesis [18–20,42–45]. Indeed, although genetic changes in PTEN result in potent Akt phosphorylation, *in vivo* studies have suggested that they show distinct phenotypes [42]. The conditional knockout of PTEN enhanced tumorigenesis in the mammary gland [43]; however, transgenic mice expressing constitutively active Akt in the mammary gland did not show tumor formation [44]. PTEN directly associates with p53, thereby increasing its stability, protein level, and transcriptional activity [18,19]. PTEN induces apoptosis and cell cycle arrest through PI3K/Akt-independent pathways [20]. PTEN also has important roles in integrin signaling and has the ability to dephosphorylate focal adhesion kinase, reducing cell adhesion and enhancing migration [46]. These findings support an alternative mechanism of PTEN-mediated tumorigenesis independent on PI3K/Akt pathway. As a second reason for the difference from *Pten* KO mice, it is possible that PI3K catalytic beta has a distinct role with PIK3CA in the phenotype of *Pten* deficiency [47].

The discrepancy between the scarce inflammatory levels in the *Pik3ca* Tg liver and the strong increase in serum ALT levels indicative of severe liver injury is to be solved in the near future. We found that inflammatory cytokine IL-1α and Fas ligand were more highly expressed in the *Pik3ca* Tg liver than in the WT liver (Supplementary Fig. 4). Taking into account reports demonstrating that these factors can lead to liver damage [28,29], it can be suggested that their abnormal upregulation in Tg livers is in part responsible for liver damage, whereas the entire molecular process inducing them remains unknown (Supplementary Fig. 13).

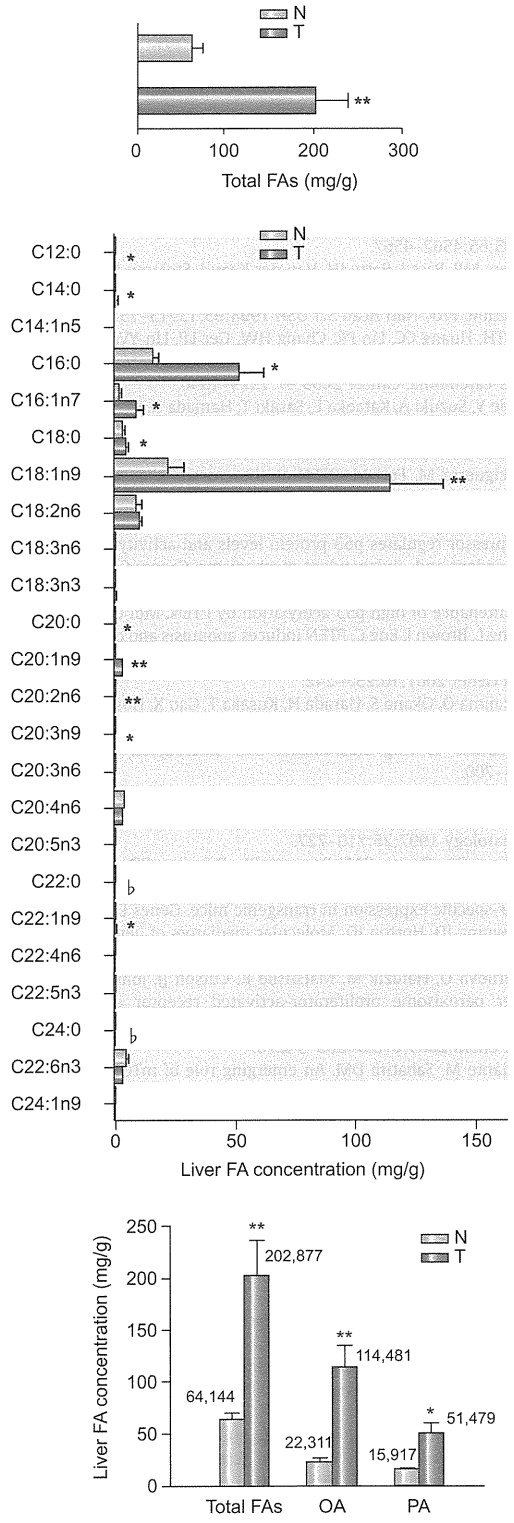

Fig. 5. The total FA composition in the *Pik3ca* Tg liver tissues and tumors. (A) The levels of FAs in the tumor (T) and non-tumor background tissue (N) in *Pik3ca* Tg mice at 52 weeks (N = 4/group; $^{**}p$ <0.01, Student's *t*-test). (B) FA composition in background (N) and tumor tissues (T) (N = 4/group; statistically increased FA levels in the tumors are shown with asterisks ($^{*}p$ <0.05, $^{**}p$ <0.01) and significantly decreased levels are shown with flat (μ, p <0.05), Student's *t*-test). (C) The concentration of total FAs, OA, and PA in background (N) and tumor tissues (T) (N = 4/group; $^{*}p$ <0.05, $^{**}p$ <0.01, Student's *t*-test).

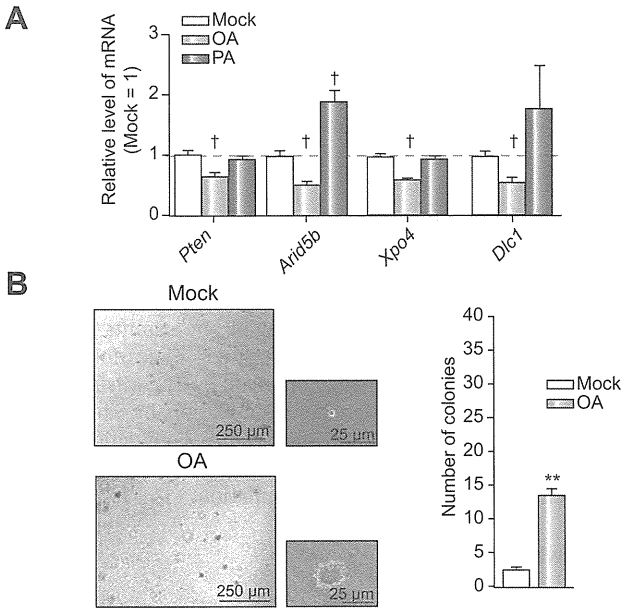

Fig. 6. OA enhances the colony-forming activity of immortalized hepatocytes. (A) OA but not PA decreased *Pten*, *Arid5b*, *Xpo4*, and *Dlc1* mRNA *in vitro* (N = 3/group; $^{\dagger}p$ <0.05, ANOVA; post hoc test with Mock group). (B) Colony formation assay of BNL-CL2 cells with or without 50 μmol/L OA in 10% or 0.5% FBS media (N = 3/group; $^{**}p$ <0.01, Student's *t*-test).

Mechanisms involved in the pathogenesis of non-alcoholic steatohepatitis (NASH) remain unclear, but the "two-hit theory" is widely accepted [48]. That is, in the first hit, insulin-resistance is followed by lipid accumulation in the liver, and the second hit, possibly involving inflammatory cytokines or oxidative stress, results in hepatic injury and fibrosis. It has been reported that ROS has certain roles in *in vivo* carcinogenesis [35], and the concentration of ROS is upregulated in the liver suffering NASH or NASH-derived HCC [49]. Regardless of the obvious fatty liver, our model mice have not shown impaired glucose tolerance. The concentration of ROS in the *Pik3ca* Tg mice was comparable with that of WT mice (Supplementary Fig. 11), which can be partly explained by the lower expression of fat-oxidative genes (Fig. 2F) and lack of inflammatory cell infiltration. These findings indicate that *Pik3ca* Tg mice do not always mimic the entire pathological mechanisms causing NASH, while they might be useful as a prototype to determine which pathological processes are required for the progression from the fatty liver to NASH. In addition, given the low rate of HCC development in these mice, they can be potentially useful for discovering tumor-promoting factors in hepatic steatosis. For example, although it was unlikely that ROS is involved in the initiation of hepatic tmor in the *Pik3ca* Tg liver, we can examine the pathological significance of ROS in tumor progression as well as hepatitis induction by applying the *Pik3ca* Tg liver to the condition producing high levels of ROS.

Recent clinical findings have advocated the relationship between volume of visceral fat and tumor progression [1–4]. While there is no direct molecular evidence to address the notion that abnormal body fat accumulation accelerates tumor growth, our data might provide new insights into the mechanisms of the "lipotoxicity-related" tumorigenesis. Future researches are needed to unravel how OA affects gene expression.

Conflict of interest

The authors who have taken part in this study declared that they do not have anything to disclose regarding funding or conflict of interest with respect to this manuscript.

Financial support

This study was supported, in part, by Health and Labor Sciences Research Grants for Research on Hepatitis from the Ministry of Health, Labor, and Welfare of Japan, by Grants-in-Aid for Scientific Research from the Ministry of Education, Culture, Sports, Science, and Technology of Japan, by The Mishima-Kaiun foundation, by the Ichiro Kanehara Foundation, by Sankyo Foundation of Life Science, by Takeda Science Foundation, by The Mochida Memorial Foundation for Medical and Pharmaceutical Research and by The Sumitomo Foundation.

Acknowledgments

We thank Dr. Richard D. Palmiter (Howard Hughes Medical Institute and Department of Biochemistry, University of Washington, Seattle, USA) and Francis V. Chisari (Department of Molecular and Experimental Medicine, Scripps Research Institute, La Jolla, USA) for providing the plasmid. We also thank Dr. Junji Shibahara (Department of Pathology, Graduate School of Medicine, The University of Tokyo) and Kojiro Ueki (Department of Metabolic Diseases, Graduate School of Medicine, The University of Tokyo) for helpful discussions, and Mitsuko Tsubouchi for technical assistance.

Supplementary data

Supplementary data associated with this article can be found, in the online version, at doi:10.1016/j.jhep.2011.03.025.

References

[1] Garfinkel L. Overweight and cancer. Ann Intern Med 1985;103:1034–1036.
[2] Deslypere JP. Obesity and cancer. Metabolism 1995;44:24–27.
[3] Schapira DV, Clark RA, Wolff PA, Jarrett AR, Kumar NB, Aziz NM. Visceral obesity and breast cancer risk. Cancer 1994;74:632–639.
[4] Yamaji Y, Okamoto M, Yoshida H, Kawabe T, Wada R, Mitsushima T, et al. The effect of body weight reduction on the incidence of colorectal adenoma. Am J Gastroenterol 2008;103:2061–2067.
[5] Hill-Baskin AE, Markiewski MM, Buchner DA, Shao H, DeSantis D, Hsiao G, et al. Diet-induced hepatocellular carcinoma in genetically predisposed mice. Hum Mol Genet 2009;18:2975–2988.
[6] Park EJ, Lee JH, Yu GY, He G, Ali SR, Holzer RG, et al. Dietary and genetic obesity promote liver inflammation and tumorigenesis by enhancing IL-6 and TNF expression. Cell 2010;140:197–208.
[7] Vinciguerra M, Carrozzino F, Peyrou M, Carlone S, Montesano R, Benelli R, et al. Unsaturated fatty acids promote hepatoma proliferation and progression through downregulation of the tumor suppressor PTEN. J Hepatol 2009;50:1132–1141.
[8] Engelman JA, Luo J, Cantley LC. The evolution of phosphatidylinositol 3-kinases as regulators of growth and metabolism. Nat Rev Genet 2006;7:606–619.
[9] Bader AG, Kang S, Zhao L, Vogt PK. Oncogenic PI3K deregulates transcription and translation. Nat Rev Cancer 2005;5:921–929.
[10] Vivanco I, Sawyers CL. The phosphatidylinositol 3-kinase AKT pathway in human cancer. Nat Rev Cancer 2002;2:489–501.
[11] Samuels Y, Diaz Jr LA, Schmidt-Kittler O, Cummins JM, Delong L, Cheong I, et al. Mutant PIK3CA promotes cell growth and invasion of human cancer cells. Cancer cell 2005;7:561–573.
[12] Lee JW, Soung YH, Kim SY, Lee HW, Park WS, Nam SW, et al. PIK3CA gene is frequently mutated in breast carcinomas and hepatocellular carcinomas. Oncogene 2005;24:1477–1480.
[13] Ikenoue T, Kanai F, Hikiba Y, Obata T, Tanaka Y, Imamura J, et al. Functional analysis of PIK3CA gene mutations in human colorectal cancer. Cancer Res 2005;65:4562–4567.
[14] Myers MP, Pass I, Batty IH, Van der Kaay J, Stolarov JP, Hemmings BA, et al. The lipid phosphatase activity of PTEN is critical for its tumor suppressor function. Proc Natl Acad Sci USA 1998;95:13513–13518.
[15] Hu TH, Huang CC, Lin PR, Chang HW, Ger LP, Lin YW, et al. Expression and prognostic role of tumor suppressor gene PTEN/MMAC1/TEP1 in hepatocellular carcinoma. Cancer 2003;97:1929–1940.
[16] Horie Y, Suzuki A, Kataoka E, Sasaki T, Hamada K, Sasaki J, et al. Hepatocyte-specific Pten deficiency results in steatohepatitis and hepatocellular carcinomas. J Clin Invest 2004;113:1774–1783.
[17] Vinciguerra M, Foti M. PTEN at the crossroad of metabolic diseases and cancer in the liver. Ann Hepatol 2008;7:192–199.
[18] Freeman DJ, Li AG, Wei G, Li HH, Kertesz N, Lesche R, et al. PTEN tumor suppressor regulates p53 protein levels and activity through phosphatase-dependent and -independent mechanisms. Cancer Cell 2003;3:117–130.
[19] Li AG, Piluso LG, Cai X, Wei G, Sellers WR, Liu X. Mechanistic insights into maintenance of high p53 acetylation by PTEN. Mol Cell 2006;23:575–587.
[20] Weng L, Brown J, Eng C. PTEN induces apoptosis and cell cycle arrest through phosphoinositol-3-kinase/Akt-dependent and -independent pathways. Hum Mol Genet 2001;10:237–242.
[21] Nakajima O, Okano S, Harada H, Kusaka T, Gao X, Hosoya T, et al. Transgenic rescue of erythroid 5-aminolevulinate synthase-deficient mice results in the formation of ring sideroblasts and siderocytes. Genes Cells 2006;11:685–700.
[22] Pasquinelli C, Shoenberger JM, Chung J, Chang KM, Guidotti LG, Selby M, et al. Hepatitis C virus core and E2 protein expression in transgenic mice. Hepatology 1997;25:719–727.
[23] Pinkert CA, Ornitz DM, Brinster RL, Palmiter RD. An albumin enhancer located 10 kb upstream functions along with its promoter to direct efficient, liver-specific expression in transgenic mice. Genes Dev 1987;1:268–276.
[24] Browning JD, Horton JD. Molecular mediators of hepatic steatosis and liver injury. J Clin Invest 2004;114:147–152.
[25] Gavrilova O, Haluzik M, Matsusue K, Cutson JJ, Johnson L, Dietz KR, et al. Liver peroxisome proliferator-activated receptor gamma contributes to hepatic steatosis, triglyceride clearance, and regulation of body fat mass. J Biol Chem 2003;278:34268–34276.
[26] Laplante M, Sabatini DM. An emerging role of mTOR in lipid biosynthesis. Curr Biol 2009;19:R1046–R1052.
[27] Patek PQ, Collins JL, Cohn M. Transformed cell lines susceptible or resistant to in vivo surveillance against tumorigenesis. Nature 1978;276:510–511.
[28] Sakurai T, He G, Matsuzawa A, Yu G-Y, Maeda S, Hardiman G, et al. Hepatocyte necrosis induced by oxidative stress and IL-1α release mediate carcinogen-induced compensatory proliferation and liver tumorigenesis. Cancer Cell 2008;14:156–165.
[29] Ogasawara J, Watanabe-Fukunaga R, Adachi M, Matsuzawa A, Kasugai T, Kitamura Y, et al. Lethal effect of the anti-Fas antibody in mice. Nature 1993;364:806–809.
[30] Gymnopoulos M, Elsliger MA, Vogt PK. Rare cancer-specific mutations in PIK3CA show gain of function. Proc Natl Acad Sci USA 2007;104:5569–5574.
[31] Aoki M, Batista O, Bellacosa A, Tsichlis P, Vogt PK. The Akt kinase: molecular determinants of oncogenicity. Proc Natl Acad Sci USA 1998;95:14950–14955.
[32] Zender L, Xue W, Zuber J, Semighini CP, Krasnitz A, Ma B, et al. An oncogenomics-based in vivo RNAi screen identifies tumor suppressors in liver cancer. Cell 2008;135:852–864.
[33] Xue W, Krasnitz A, Lucito R, Sordella R, Vanaelst L, Cordon-Cardo C, et al. DLC1 is a chromosome 8p tumor suppressor whose loss promotes hepatocellular carcinoma. Genes Dev 2008;22:1439–1444.
[34] Zeng Q, Hong W. The emerging role of the hippo pathway in cell contact inhibition, organ size control, and cancer development in mammals. Cancer Cell 2008;13:188–192.
[35] Ishii H, Horie Y, Ohshima S, Anezaki Y, Kinoshita N, Dohmen T, et al. Eicosapentaenoic acid ameliorates steatohepatitis and hepatocellular carcinoma in hepatocyte-specific Pten-deficient mice. J Hepatol 2009;50:562–571.

[36] Suganami T, Tanimoto-Koyama K, Nishida J, Itoh M, Yuan X, Mizuarai S, et al. Role of the Toll-like receptor 4/NF-kappaB pathway in saturated fatty acid-induced inflammatory changes in the interaction between adipocytes and macrophages. Arterioscler Thromb Vasc Biol 2007;27:84–91.
[37] Vinciguerra M, Veyrat-Durebex C, Moukil MA, Rubbia-Brandt L, Rohner-Jeanrenaud F, Foti M. PTEN down-regulation by unsaturated fatty acids triggers hepatic steatosis via an NF-kappaBp65/mTOR-dependent mechanism. Gastroenterology 2008;134:268–280.
[38] Vinciguerra M, Sgroi A, Veyrat-Durebex C, Rubbia-Brandt L, Buhler LH, Foti M. Unsaturated fatty acids inhibit the expression of tumor suppressor phosphatase and tensin homolog (PTEN) via microRNA-21 up-regulation in hepatocytes. Hepatology 2009;49:1176–1184.
[39] Hatanaka H, Tsukui M, Takada S, Kurashina K, Choi YL, Soda M, et al. Identification of transforming activity of free fatty acid receptor 2 by retroviral expression screening. Cancer Sci 2010;101:54–59.
[40] Kang S, Bader AG, Vogt PK. Phosphatidylinositol 3-kinase mutations identified in human cancer are oncogenic. Proc Natl Acad Sci USA 2005; 102:802–807.
[41] Pettinelli P, Videla LA. Up-regulation of PPAR-γ mRNA expression in the liver of obese patients: an additional reinforcing lipogenic mechanism to SREBP-1c induction. J Clin Endocrinol Metab 2011;96:1424–1430.
[42] Blanco-Aparicio C, Renner O, Leal JF, Carnero A. PTEN, more than the AKT pathway. Carcinogenesis 2007;28:1379–1386.
[43] Li G, Robinson GW, Lesche R, Martinez-Diaz H, Jiang Z, Rozengurt N, et al. Conditional loss of PTEN leads to precocious development and neoplasia in the mammary gland. Development 2002;129:4159–4170.
[44] Ackler S, Ahmad S, Tobias C, Johnson MD, Glazer RI. Delayed mammary gland involution in MMTV-AKT1 transgenic mice. Oncogene 2002;21: 198–206.
[45] Hutchinson J, Jin J, Cardiff RD, Woodgett JR, Muller WJ. Activation of Akt (protein kinase B) in mammary epithelium provides a critical cell survival signal required for tumor progression. Mol Cell Biol 2001;21:2203–2212.
[46] Tamura M, Gu J, Matsumoto K, Aota S, Parsons R, Yamada KM. Inhibition of cell migration, spreading, and focal adhesions by tumor suppressor PTEN. Science 1998;280:1614–1617.
[47] Jia S, Liu Z, Zhang S, Liu P, Zhang L, Lee SH, et al. Essential roles of PI(3)K-p110beta in cell growth, metabolism and tumorigenesis. Nature 2008;454: 776–779.
[48] Day CP, James OF. Steatohepatitis: a tale of two "hits"? Gastroenterology 1998;114:842–845.
[49] Malaguarnera L, Madeddu R, Palio E, Arena N, Malaguarnera M. Heme oxygenase-1 levels and oxidative stress-related parameters in non-alcoholic fatty liver disease patients. J Hepatol 2005;42:585–591.

Hepatology Research

Hepatology Research 2011; 41: 1199–1207 doi: 10.1111/j.1872-034X.2011.00871.x

Original Article

Diagnostic accuracy of α-fetoprotein and des-γ-carboxy prothrombin in screening for hepatocellular carcinoma in liver transplant candidates

Noriyo Yamashiki,[1] Yasuhiko Sugawara,[2] Sumihito Tamura,[2] Junichi Kaneko,[2] Haruhiko Yoshida,[1] Taku Aoki,[2] Kiyoshi Hasegawa,[2] Masaaki Akahane,[3] Kuni Ohtomo,[3] Masashi Fukayama,[4] Kazuhiko Koike[1] and Norihiro Kokudo[2]

[1]*Department of Gastroenterology,* [2]*The Artificial Organ and Transplantation Division, Department of Surgery,* [3]*Department of Radiology, and* [4]*Department of Pathology, Graduate School of Medicine, The University of Tokyo, Tokyo, Japan*

Aim: Although hepatocellular carcinoma (HCC)-specific serum tumor markers, α-fetoprotein (AFP) and des-γ-carboxy prothrombin (DCP), are used in the screening for HCC, their utility in pre-transplantation evaluation is not well established. This study aimed to evaluate the accuracy of AFP and DCP measurement for the diagnosis of HCC in liver transplant candidates.

Methods: A total of 315 consecutive adult patients (174 men and 141 women, mean age 52 years), who were to receive liver transplantation for end-stage liver diseases, were enrolled. The pre-transplant levels of AFP and DCP were compared with the histopathology of explanted liver.

Results: Hepatocellular carcinoma was present in the explanted liver of 106 recipients (median number of nodules 2, mean diameter 2.5 cm). The area under receiver operating characteristic curve for the diagnosis of HCC was 0.83 (95% confidence interval, 0.78–0.88) for AFP and 0.47 (0.41–0.54) for DCP. With the cut-off value of 100 mAU/mL, 20/106 (18.9%) patients with HCC and 54/194 (27.8%) patients without HCC were positive for DCP. DCP positivity was associated with vascular invasion, tumor differentiation and size among patients with HCC, which was associated with albumin level among patients without HCC. Vitamin K was administered prior to transplantation to 20 patients who were positive for DCP (two with and 18 without HCC), resulting in a decrease in DCP levels in 19 of them.

Conclusions: Serum DCP levels may be raised in end-stage liver disease patients without HCC, and cannot be used as a reliable marker for HCC among liver transplant candidates.

Key words: hepatocellular carcinoma, sensitivity and specificity, tumor marker, vitamin K deficiency

INTRODUCTION

CIRRHOSIS WITH EARLY-STAGE hepatocellular carcinoma (HCC) is currently one of the leading indications for liver transplantation. The introduction of the Milan criteria, i.e., a single tumor up to 5 cm in size or as many as three tumors up to 3 cm in size, and no vascular invasion has led to low incidence of recurrence post-transplantation in various transplant centers around the world.[1] The Milan criteria have now been adopted as the selection criteria for liver transplantation in the United States, Europe, and Japan.[2–4] Expanded criteria, such as the UCSF criteria or Tokyo rule, are proposed by several groups,[5,6] although the superiority of expanded criteria over Milan criteria is controversial.[7] Nevertheless, survival is reported to be poorer after liver transplantation for more advanced HCC outside the criteria, it is important to detect early-stage HCC that meets the eligibility requirements for liver transplantation.

In the screening for HCC, α-fetoprotein (AFP) measurement is widely used in conjunction with imaging studies, although the use of this marker alone has relatively low sensitivity (39–71%) and specificity (49–91%).[8,9] Other serum markers, such as des-γ-carboxy prothrombin (DCP) and the lens culinaris

Correspondence: Dr Yasuhiko Sugawara, Department of Surgery, Artificial Organ and Transplantation Division, Graduate School of Medicine, The University of Tokyo, 7-3-1 Hongo, Bunkyo-ku, Tokyo 113-8655, Japan. Email: yasusuga-tky@umin.ac.jp
Received 20 March 2011; revision 17 June 2011; accepted 5 July 2011.